Materials Today Advances 5 (2020) 100055

Contents lists available at ScienceDirect

Materials Today Advances

journal homepage: www.journals.elsevier.com/materials-today-advances/

Cellulose nanocrystals in smart and stimuli-responsive materials: a review

R. Nasseri [a, b, c], C.P. Deutschman [a, b, c], L. Han [a, b], M.A. Pope [a, b, **], K.C. Tam [a, b, *]

[a] Department of Chemical Engineering, University of Waterloo, 200 University Avenue West, Waterloo, Ontario, N2L 3G1, Canada
[b] Waterloo Institute for Nanotechnology, University of Waterloo, 200 University Avenue West, Waterloo, Ontario, N2L 3G1, Canada

ARTICLE INFO

Article history:
Received 2 October 2019
Received in revised form
19 December 2019
Accepted 8 January 2020
Available online 14 February 2020

Keywords:
Sustainable nanomaterials
Smart materials
Polymers
Hybrid systems

ABSTRACT

"Smart" stimuli-responsive materials have been the subject of decades of research because of their versatility and particularly their use in medical and sensing applications. While these materials are often composed exclusively of responsive polymers, there is growing interest in smart hybrid systems that contain at least two distinct components, each contributing uniquely to the final material. Cellulose nanocrystals (CNCs) have found extensive application in smart hybrid systems, as CNCs can both contribute to the mechanical and optical properties of the system and bear stimuli-responsive surface modifications. This review covers the recent body of work on CNC-containing smart hybrid systems, with attention given to the fabrication methodologies that have been employed to generate both physically and optically adaptable CNC-based smart systems. Additionally, the unique application of CNCs in self-healing composites and shape memory polymers will be discussed.

1. Introduction

A desirable trait inherent to many biological materials is their ability to respond dynamically to a specific stimulus or a suite of stimuli. This dynamic response is manifested as a predictable change in some key properties (such as the color of an octopus' skin or the shape of a plant's leaves) over time. In contrast to biological systems, many synthetic materials are static, limiting their range of applications and their tolerance for change [1]. Smart materials, as defined for the purpose of this review, are materials designed to possess at least one property that changes reproducibly in response to at least one stimulus. These materials have been the subject of decades of research because of their improved versatility when compared to traditional synthetic materials. Smart materials may respond to a wide range of stimuli, including changes in temperature, light, mechanical stress, or environmental pH [2].

A vast number of smart materials are based on smart polymers, which most often derive their responsive character from the properties of the incorporated moieties [3]. Subtle changes in the state of these compounds, such as volumetric or conformational changes in the polymer chain, will result in macroscopic changes in the material. Among these macroscopic changes are variations in physical state, such as swelling or stiffening [4], or changes in phase, such as solution-to-gel or gel-to-solution transitions [5]. Sensitivity to changes in pH, for example, may be achieved using polymer chains composed of weak polyelectrolytes (i.e., poly(-acrylic acid) (PAA) or poly(N,N-dimethylaminoethyl methacrylate)), which will transform from a collapsed to a swollen or rod-like conformation when ionized [6–8]. Alternatively, light sensitivity can be derived from the addition of light-activated moieties, such as azobenzene groups, which undergo reversible photo-isomerization between stable *trans* and less stable *cis* isomers [9]. In summary, a rational design of the polymer architecture and functionalization is what endows smart materials with their predictable and dynamic properties.

In addition to smart polymers, the generation of smart hybrid systems allows for even greater functionality to be achieved. For the purpose of this review, smart hybrid systems can be defined as a category of smart materials that combine a stimuli-responsive component (most frequently a smart polymer) with at least one other component that alters the responsive behavior or provides the system with additional desired properties. For instance, smart systems with targeted bioactivity have been fabricated by conjugating smart polymers to biomacromolecules or proteins [10,11].

* Corresponding author.
** Corresponding author.
E-mail addresses: michael.pope@uwaterloo.ca (M.A. Pope), mkctam@uwaterloo.ca (K.C. Tam).
[c] Note: Nasseri and Deutschman made equal contributions.

https://doi.org/10.1016/j.mtadv.2020.100055

Alternatively, inorganic components, such as gold nanoparticles, can be incorporated into smart polymer matrices to design materials with tunable optical properties [12]. In recent years, a large body of work has been devoted specifically to smart hybrid systems containing cellulose nanocrystals (CNCs), and these smart cellulose-based systems are the focus of the present review.

CNCs are rod-like nanoparticles extracted from plants and agricultural biomass, and they are particularly well-suited for application in smart systems. They are sustainable and biodegradable resources that can be surface modified with functional groups with specific functionality [13–15]. There are many sources of cellulose, including wood fibers, tunicates, and some species of bacteria [16]. The nanocrystals can be derived from cellulosic precursors via acid hydrolysis, sonochemical fragmentation, microbial or enzymatic digestion, and other top-down fabrication methods [17–19]. The source and extraction method dictate the exact morphology of the CNCs produced, and they generally possess lateral and length dimensions of 3–5 nm and 100–300 nm, respectively [20,21]. CNCs also possess desirable mechanical characteristics, such as high surface area (~250 m^2/g), high tensile strength (7500 MPa), and high stiffness (Young's modulus up to 140 GPa) [22]. Additionally, there is an abundance of reactive surface hydroxyl groups on the C6 of the D-glucose units, providing a facile platform for chemical modifications to yield functionalized CNCs that can be readily integrated into smart hybrid systems [23].

Most of the recent work on smart CNC hybrid systems can be grouped into four categories. The first area is physically adaptive systems, whose physical state changes in response to specific external stimuli, and CNCs often provide the platform needed to add this functionality to the system [24–26]. The second group of materials includes optically adaptable systems, where the incorporation of CNC yields chiral nematic films that reflect different wavelengths of light depending on applied environmental stimulus [27]. The last two groups of smart CNC hybrid systems, self-healable CNC composites and CNC-based shape memory polymers, represent some of the most advanced applications of smart and functional materials [28,29]. The present review examines the impact and advantages of using CNCs in each of these four groups of smart systems and highlights trends in the fabrication techniques used and the most common areas of application.

2. Physically adaptable smart systems

2.1. Thermo-responsive adaptable systems

One of the most conventional and well-studied stimuli used to control smart polymeric systems is heat. Thermo-responsive polymers contain both hydrophobic and hydrophilic segments and will exist in either an extended chain or a collapsed globule conformation, depending on the thermal state of the system. These systems can be described by a lower critical solution temperature (LCST) or an upper critical solution temperature (UCST) depending on whether the polymer collapses or extends with increasing temperature [30]. The difference between the two is illustrated in Fig. 1. In the case of LCST polymers, such as poly(N-isopropylacrylamide) (PNIPAM), the brush-to-globule transition occurs with increasing temperatures because of unfavorable interactions between the polymer and surrounding water molecules, as well as increasing intra-polymer hydrogen bonding [25]. This leads to a reversible collapse, or aggregation, of the polymer chains, resulting in a dramatic reduction in solubility [2].

By combining the unique properties of CNCs with thermo-responsive polymers, more advanced, physically adaptable smart systems can be prepared. An overview of recently developed thermo-responsive/CNC systems is summarized in Table 1. Three strategies have been employed to produce these hybrid systems—"grafting to" polymerization [31–36], "grafting from" polymerization [32,37–39], and physical mixing [40–42]. The "grafting to" and "grafting from" methods both allow the polymer brushes to be covalently anchored to the surface of the CNC. With the "grafting to" technique, well-defined and well-characterized polymer brushes can be synthesized and subsequently attached to the surface of CNCs. This method provides more flexibility in how the polymers are synthesized prior to attachment and allows for the use of commercial polymers. However, steric hindrance restricts the maximum achievable grafting density with the "grafting to" technique, as unattached polymer chains must diffuse through already grafted brushes to reach the reactive sites [43]. In order to increase the grafting density, the "grafting from" method can be employed. In this approach, initiator molecules are first attached to the surface of CNCs, and then monomer precursors are added to the system, which are polymerized directly from the initiator sites [37,44]. Higher grafting density can be achieved because of the easier diffusion of monomers to the active sites, even when many polymer chains have already been formed. Table 1 provides an overview of the fabrication techniques that have recently been used to generate CNC/thermo-responsive polymer hybrid systems. Some of the specific hybrid systems are discussed in more detail in the remainder of this section, with an emphasis on the fabrication methodologies and proposed applications.

Cudjoe et al. [31] designed a nanocomposite consisting of CNC, grafted with a LCST polymer and subsequently embedded within a poly(vinyl acetate) (PVAc) matrix. The amine-end-capped poly[2-(2-(2-methoxyethoxy)ethoxy)ethyl acrylate] (POEG3A) (LCST of 60 °C) was grafted to carboxylated CNCs to yield a thermo-responsive nanocomposite. Below the LCST, the grafted polymer chains disrupt the interaction between individual cellulose nanoparticles, limiting their reinforcing effect. However, upon exposure to water above the LCST, the grafted chains undergo a coil-to-globule transition, reducing the inter-particle separation of CNCs that stiffen the nanocomposite as the CNCs form a percolating network.

Thérien-Aubin and coworkers [38] developed a temperature-responsive hydrogel with capability of on-demand formation and dissociation under physiological conditions. This was achieved through the grafting of thermo-responsive copolymer chains of N-isopropylacrylamide (NIPAM) and N,N′-dimethylaminoethyl methacrylate (DMAEMA) from the surface of CNC via RAFT polymerization. Upon heating of the CNC-g-NIPAM-DMAEMA suspension above the LCST, the increased intramolecular association of grafted copolymers leads to gel formation. The gelation temperature of the CNC-g-NIPAM-DMAEMA suspension was tuned to 37 °C by tailoring the copolymer composition on the surface of CNC. The thermo-reversible gels were employed for cell encapsulation and culturing that displayed low cytotoxicity. Reducing the temperature led to the dissociation of the gel, enabling cell release. In another work, the same group employed a similar temperature-responsive hydrogel as an extracellular matrix for the growth of three-dimensional cancer spheroids [49]. They successfully cultured MCF-7 breast cancer cells into cancer spheroids by dispersing them in a suspension of CNC-g-PNIPAM in a cell culture medium. By heating to 37°C (above the LCST of PNIPAM), the solution gelled, and the cell growth was enhanced. Similar size, shape, and growth profiles were observed for cancer spheroids grown in this hydrogel as in Matrigel, a standard medium for cancer spheroid culture. The advantage of the thermo-responsive characteristic of this hydrogel is that the cancer spheroids could be released by cooling the hydrogel, as shown in Fig. 2A. This allows for the tumorigenic properties of the released cancer spheroids to be further examined,

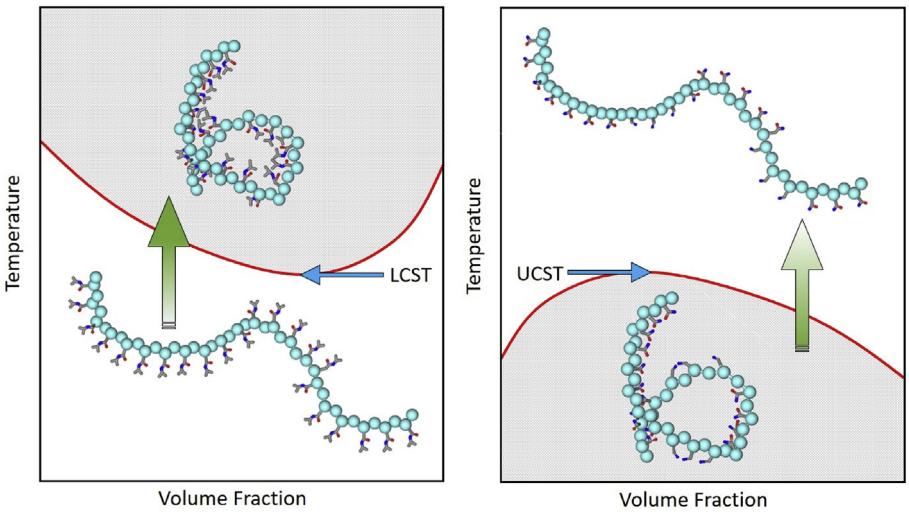

Fig. 1. Schematic illustration of the transition behavior of LCST and UCST thermo-responsive polymers; the red line represents the macroscopic phase transition. The left panel shows the behavior of an LCST polymer, such as poly(N-isopropylacrylamide) in water, and the right panel shows the behavior of a UCST polymer, such as poly(acrylamide-co-acrylonitrile) in water [31].

Table 1
Recent techniques for incorporating CNCs into thermo-responsive hybrid systems.

Fabrication Method	Polymer	Ref.
Grafting From CNCs		
ATRP	Poly(oligo(ethylene glycol)) methacrylate	[37]
ATRP	Poly[2-(2-(2-methoxyethoxy)ethoxy)ethyl acrylate]	[31]
AGET-ATRP	Poly(N-isopropylacrylamide) and 4-ethoxy-9-allyl1,8-naphthalimide	[45]
SI-ATRP	Poly(poly(ethylene glycol) methylacrylate)	[39]
FRP	Poly(N-isopropylacrylamide)	[46]
RAFT	Poly(N-isopropylacrylamide) and Poly(N,N′-dimethylaminoethyl methacrylate)	[38]
LRP	Poly(N-isopropylacrylamide-co-stearyl methacrylate)	[47]
Grafting To CNs		
Peptide Coupling	Jeffamine polyetheramines M2005 and T5000	[34]
Peptide Coupling	Jeffamine polyetheramine M2005	[33]
Mixing with CNCs		
H-Bonding	Poloxamer 407	[40]
H-Bonding	Poly(N-isopropylacrylamide) and triethylene glycol dimethacrylate (crosslinker)	[41]
Hydrophobic Bonding	Hydroxypropyl methylcellulose	[42]
Electrostatic Attraction	Poly(2-(dimethylamino)ethyl methacrylate) and Poly(di(ethylene glycol) methyl ethermethacrylate)	[48]

**Key: ATRP, Atom Transfer Radical Polymerization; AGET-ATRP, Activators Generated by Electron Transfer for ATRP; SI-ATRP, Surface Initiated-Atom Transfer Radical Polymerization; FRP, Free Radical Polymerization; RAFT, Reversible Addition−Fragmentation Chain-Transfer Polymerization.

benefiting fundamental cancer research and cancer drug screening research.

Zubik et al. also synthesized a CNC-g-PNIPAM thermo-responsive hydrogel, with potential application in wound dressing [46]. Increasing the CNC content of the hybrid system led to an improvement in the mechanical stability of the hydrogel, while clear thermo-responsive behavior (with the transition temperature in the range of 36−39°C) was maintained. To evaluate the potential of this hydrogel for wound dressing, antibiotic and antiprotozoal compounds were loaded into the hydrogel at room temperature, and the drug release profile at 37 °C was investigated. The authors found that the system produced a burst release, followed by a slow and sustained release, which is well suited for wound treatment applications.

Gicquel and coworkers reported on the electrostatic adsorption of a block copolymer onto oxidized cellulose nanocrystals (TO-CNCs) to prepare a solution with temperature-dependent rheological properties [48]. The block copolymer, composed of a cationic poly(2-(dimethylamino)ethyl methacrylate) (PDMAEMA) block and a thermo-responsive poly(di(ethylene glycol) methyl ether methacrylate) (PDEGMA) block, was synthesized using ATRP. The cationic block copolymer and highly anionic TO-CNCs were prepared in an aqueous solution at a 4:1 ratio yielding individually coated CNC particles. Upon heating above the LCST of the thermo-responsive block, interparticle association was enhanced. leading to the aggregation of the modified CNCs, while the non-adsorbed polymers bridged the aggregates, converting the solution to a more viscous hydrogel.

Lee et al. employed surface-mediated living radical polymerization to graft poly(N-isopropylacrylamide-co-stearyl methacrylate) (poly(NIPAM-co-SMA)) brushes onto the CNC, yielding a thermo-responsive rheology modifier [47]. By changing the ratio of NIPAM to SMA grafted to the CNC, the strength of the hydrophobic interactions could be manipulated. Above the LCST of PNIPAM, the enhanced hydrophobic interactions induced the interparticle association that resulted in the increase of viscosity, storage, and loss modulus of the solution containing the modified CNC.

Lin and coworkers have also fabricated thermo-responsive CNC-based rheology modifiers [34]. Two commercial thermo-sensitive polyetheramines, Jeffamine M2005 and Jeffamine T5000, were grafted to the reducing end of CNC using a two-step protocol

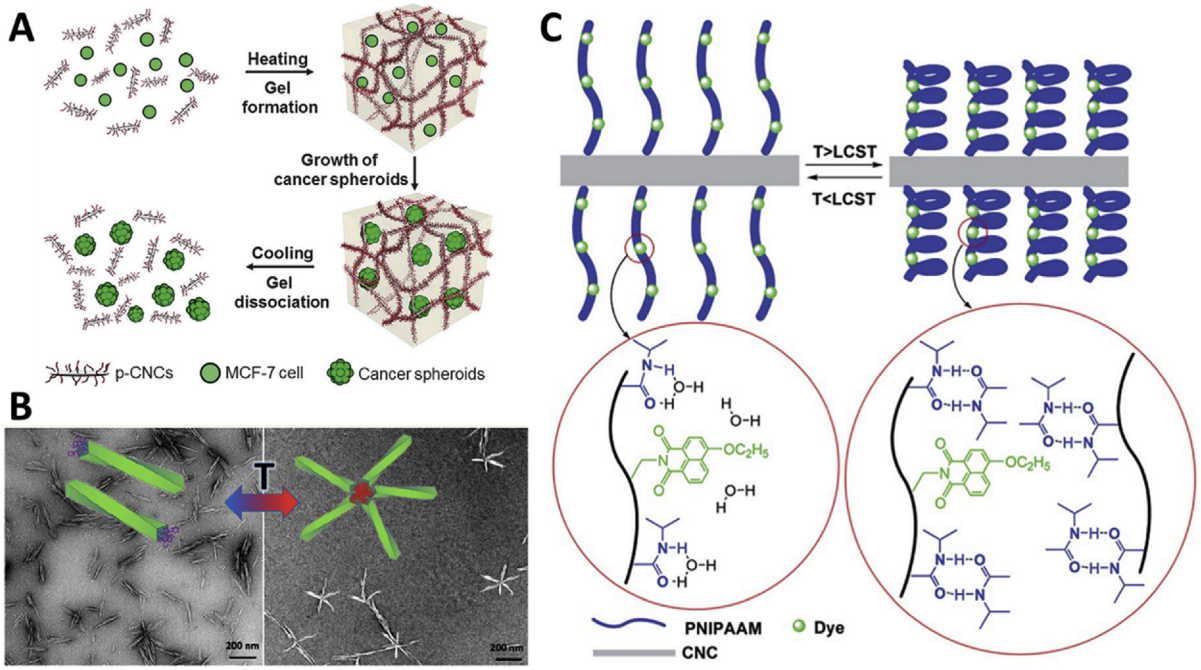

Fig. 2. (A) Encapsulation, growth, and release of cancer spheroids from the CNC-g-PNIPAM (p-CNCs) hydrogel [49]. (B) Thermo-reversible association of CNC-g-polyetheramine into highly symmetric star-shaped assemblies [34]. (C) Conformational changes of grafted PNIPAM brushes below and above the LCST [45].

involving an end carboxylation followed by a peptide coupling with the primary amine moiety on the polyetheramine. Upon heating above the LCST of polyetheramine (~16°C), association of the derivatized ends pulls the CNC particles together into highly symmetric four-, five-, or six-branched star shapes, as shown in Fig. 2B. The thermal reversibility and specific physicochemical characteristics of the generated CNC/polymer material offer a powerful and biocompatible tool to modify the rheological properties of biological systems.

Nigmatullin et al. synthesized hydrophobized CNC for potential application as a rheology modifier by surface binding octylamine to the CNC. The hydrophobized CNC was then mixed with hydroxypropyl methylcellulose (HPMC) to produce a thermo-responsive hydrogel [42]. Upon increasing the temperature, the association of hydrophobic moieties causes entropically driven release of ordered/bound water resulting in the increase in viscosity and storage modulus of the hydrogel. The relative contents of the soluble polymer and octyl-CNC were manipulated to control the rheological properties of hydrogel, allowing the control of the viscosity for a given application.

Zoppe et al. reported on the synthesis of PNIPAM brushes grafted from CNCs via surface-initiated single-electron transfer living radical polymerization (SI-SET-LRP) [50]. The CNC-g-PNIPAM system was used as a switchable stabilizer for water-in-oil Pickering emulsions. At temperatures below the LCST of the system, it acts as an effective emulsifier, as the CNC stabilizes the oil–water interface. However, upon heating above the LCST of the grafted PNIPAM, the brushes collapse, inducing the aggregation of the emulsion droplets. This forces the CNC to desorb from the oil–water interface, and the emulsions subsequently break.

Wu et al. grafted PNIPAM from the surface of CNC using electron transfer for atom transfer radical copolymerization (AGET-ATRP) of NIPAM and a polymerizable fluorescent dye, 4-ethoxy-9-allyl-1,8-naphthalimide (EANI), to form a thermo-responsive system that could function as a drug carrier, a fluorescent probe, or a sensor [45]. When the temperature was increased beyond the LCST of the grafted NIPAM brushes, the CNC-g-PNIPAM-co-EANI suspension showed an improved fluorescence intensity, when compared to a pure EANI solution. According to the authors, an increase in temperature would normally reduce the fluorescent efficiency of EANI, because of an increase in non-radiative transitions of the dye. However, when EANI is attached to CNC with PNIPAM, the collapse of the copolymer brushes at higher temperatures inhibits the rotation and vibration of dye molecules, decreasing the non-radiative transition of dye, and increases its fluorescence intensity. This change in physical interaction is shown in Fig. 2C.

Wu et al. used AGET-ATRP to copolymerize NIPAM and two polymerizable fluorescent dyes, EANI and 4-methylamino-9-allyl-1,8-naphthalimide (MANI), from the surface of CNC for potential application in smart drug delivery [51]. By using CNC as the base for copolymerization, a system that is both fluorescent (and therefore traceable within tissues and organs) and drug carrying was produced. The authors investigated the loading and release of 5-fluorouracil, a common anti-cancer drug, from the grafted CNC system, and found that increasing the temperature above the LCST of PNIPAM allowed for an increased release of the drug.

Larsson et al. fabricated a cryogel of PNIPAM by free radical cryopolymerization of NIPAM in the presence of polymerizable acrylate-functionalized CNC [4]. As cryo-polymerization was performed below the freezing point of the solvent, the majority of the solvent formed crystals, leaving only a liquid microphase, where the reactants were concentrated and polymerization occurred. After polymerization, an interconnected, macroporous structure remained upon thawing. The cryogel with polymerizable CNC possessed a good de-swelling/swelling response upon heating beyond the LCST and cooling below the LSCT of PNIPAM, as well as a higher tolerance for compressive strain before breaking.

Sun et al. prepared a thermo-responsive hydrogel by UV initiated free radical polymerization and cross-linking of NIPAM in the presence of CNC, for potential application in thermally responsive and tunable optical devices [41]. The authors proposed that increasing the temperature above the LCST leads to the dehydration

of PNIPAM, which induces light scattering and changes the material from transparent to opaque. Although the PNIPAM/CNC hydrogel with high water content showed a similar LCST to PNIPAM, increasing the amount of CNC reduced the LCST in hydrogels with low water content. This suggests that variation of the amount of CNC could allow the low water content gels to be tuned to one with a LCST compatible for any given application.

2.2. pH-responsive adaptable systems

Because of the versatile applications of CNC in colloidal and aqueous dispersion systems, there has been extensive interest in the development of CNC-based pH-responsive smart systems. When the properties of a material or its interaction with the surrounding changes with the variation of proton concentration, it can be considered pH-responsive [52]. Three basic techniques have been exploited to prepare pH-responsive CNC systems: i) modification of the surface of CNC with functional groups, such as carboxylate groups and amine groups, yielding negative and positive surface charges when deprotonated or protonated in an aqueous solution [53–55]; ii) the direct incorporation of CNC into polymers such as polyelectrolytes that are inherently pH-responsive [56]; and iii) grafting of polymers to the CNC surface using pH-sensitive linkages, such as C=N bonds [57]. In all three cases, the CNC provides the primary platform for pH sensitivity to be introduced to the system, while allowing for additional modifications via the incorporation of copolymers. Because of this flexibility, CNC-based pH-responsive systems have a wide range of potential applications, including water treatment, food engineering, biomedicine, and pharmaceuticals.

Pickering emulsions are one of the most important applications of CNC-based pH-responsive systems. Compared to traditional emulsions that use surfactants, Pickering emulsions have advantages, such as low cost, easy recovery, and better eco-compatibility. pH-responsive CNC-based Pickering emulsifiers have even further advantages, as they can cause alternate stabilization and destabilization of emulsions in response to variations in pH. Additionally, because the CNC-based emulsifiers can desorb selectively from the emulsion interface, these hybrid systems can be readily recovered and reused.

Many of the responsive Pickering emulsions rely on CNCs grafted with pH-responsive polymer brushes. For example, Tang et al. [58] reported on a pH-responsive Pickering emulsion stabilized by poly[2-(dimethylamino)ethyl methacrylate] (PDMAEMA) grafted CNCs. The hydrophobicity of the synthesized polymer brushes was altered in low and high pH due to the protonation and deprotonation of PDMAEMA chains, which led to the emulsification and demulsification of oil droplets, as shown in Fig. 3A. Zhou et al. [35] reported on a CNC/fluorinated polyarylated soap-free emulsion. The surface functionalized CNCs were grafted with two different polymers: poly(2-(dimethylamino) ethyl methacrylate) (PDMAEMA) and poly(2,2,3,4,4,4-hexafluorobutyl acrylate) (PHFBA). The hydrophobic PHFBA chain and hydrophilic PDMAEMA chain controlled the wettability of the CNC Pickering emulsifier. At a pH of 1, the protonated PDMAEMA was more hydrophilic, inducing the coalescence of the oil droplets. With increasing pH, the size of oil droplets decreased significantly because of the increased hydrophobicity and then slightly increased due to the change in surface charge density.

Apart from grafting pH-responsive polymers, CNC emulsifiers can be prepared by conjugating hydrophobic chains to the CNC surface with a pH-sensitive linkage. Du et al. [57] reported on a Pickering emulsion stabilized by functionalized CNC with pH-triggered demulsification behavior, where a 18-carbon alkyl chain was grafted to CNC via a C=N bond. Because of the hydrophobicity of the grafted alkyl chains, the Pickering emulsion possessed good stability. At a pH lower than 4.0, the functionalized CNC became hydrophilic due to the removal of the C=N bond linkages, which led to the demulsification of the Pickering emulsion. Li et al. [56] reported on the preparation and stabilization of Pickering emulsion using the formation and assembly of CNC surfactants at the water–oil interface. CNC and amine-terminated polystyrene ($PS-NH_2$) were utilized to form pH-responsive CNC surfactants that are controlled by changing the electrostatic interactions between the polymer chain ends and CNCs. At a pH of 3 (above the pK_a of sulfate groups on CNC (~1.9) and below the pK_a of amine groups (~9.0)), the deprotonated CNC sulfate groups and protonated polymer amine groups displayed strong electrostatic interactions at the interface, which effectively reduced the interfacial tension, as shown schematically in Fig. 3B(a). When the pH value was increased, the average size of the emulsion droplets increased due to the reduced capability of CNC surfactants to lower the interfacial tension, as shown in Fig. 3B(b, c, and d). Other pH-responsive Pickering emulsions were developed with various types of CNC nanohybrids. Low et al. [59] studied the pH-responsive Pickering emulsion stabilized by Fe_3O_4–CNC nanocomposites. By adjusting the pH, the hydrophobicity of the Fe_3O_4–CNC nanocomposites can be tuned and thus the stability of the Pickering emulsion could be controlled.

Apart from their use in Pickering emulsions, manipulating the surface charge and hydrophobicity of functionalized CNC could also alter the dispersity or colloidal stability, opening up other applications, such as flocculation in industrial processes. Kan et al. [60] reported on poly(4-vinylpyridine)-grafted CNC (CNC-g-P4VP) that displayed pH-responsive flocculation and sedimentation capabilities. P4VP was grafted onto CNCs via the surface-initiated polymerization with ceric(IV) ammonium nitrate and the stability of CNC-g-P4VP was controlled by adjusting pH and tuning the hydrophilic properties of the CNC. Under acidic conditions, CNC-g-P4VP exhibited excellent stability in water. At pH > 5, the pyridyl groups on the P4VP chains were deprotonated and CNC-g-P4VP became hydrophobic and precipitated in aqueous solution. This process was visually observable in 0.004 wt% aqueous solution and was reversible. Zhang et al. [61] synthesized a pH-responsive P4VP-g-CNC that was used to stabilize gold nanoparticle (Au NPs) nanocatalysts. At pH lower than 5, Au@CNC-g-P4VP acted as an efficient nanocatalyst, while at pH greater than 5, this nanocatalyst could be recovered via flocculation.

Garcia-Valdez and coworkers [5] also developed pH-responsive polymer-grafted CNCs. Three different CO_2-(pH)-responsive polymers, poly[2-(dimethylamino)ethyl methacrylate] (PDMAEMA), 2-(diethylamino)ethyl methacrylate (DEAEMA), and poly(N-[3-(dimethylamino)propyl]) methacrylamide (PDMAPMAm), were grafted onto CNCs through surface-initiated nitroxide-mediated polymerization (SI-NMP). While pristine CNCs were only dispersible in water and polar solvents, these polymer-grafted CNCs were dispersible in both polar and nonpolar solvents due to their adjustable hydrophobicity/hydrophilicity with pH when subjected to CO_2/N_2 bubbling. For example, PDEAEMA is hydrophilic in its protonated state and hydrophobic when deprotonated below the p*Ka* of 7.3. Thus, CNC-g-PDEAEMA displayed high dispersibility at low pH and aggregated after purging with N_2, as shown in Fig. 2C. It was demonstrated that this change between dispersed solution phase and aggregate gel phase was highly cyclable.

In another work, Glasing et al. [36] reported on two pH-responsive surface functionalized CNCs via the grafting of CNC with PDEAEMA and PDMAPMAm. The effect of grafting density and molecular weight of two types of tertiary amine polymer-grafted CNCs were investigated. It was suggested that the pH-responsive switching of CNC from a hydrophilic to a hydrophobic state

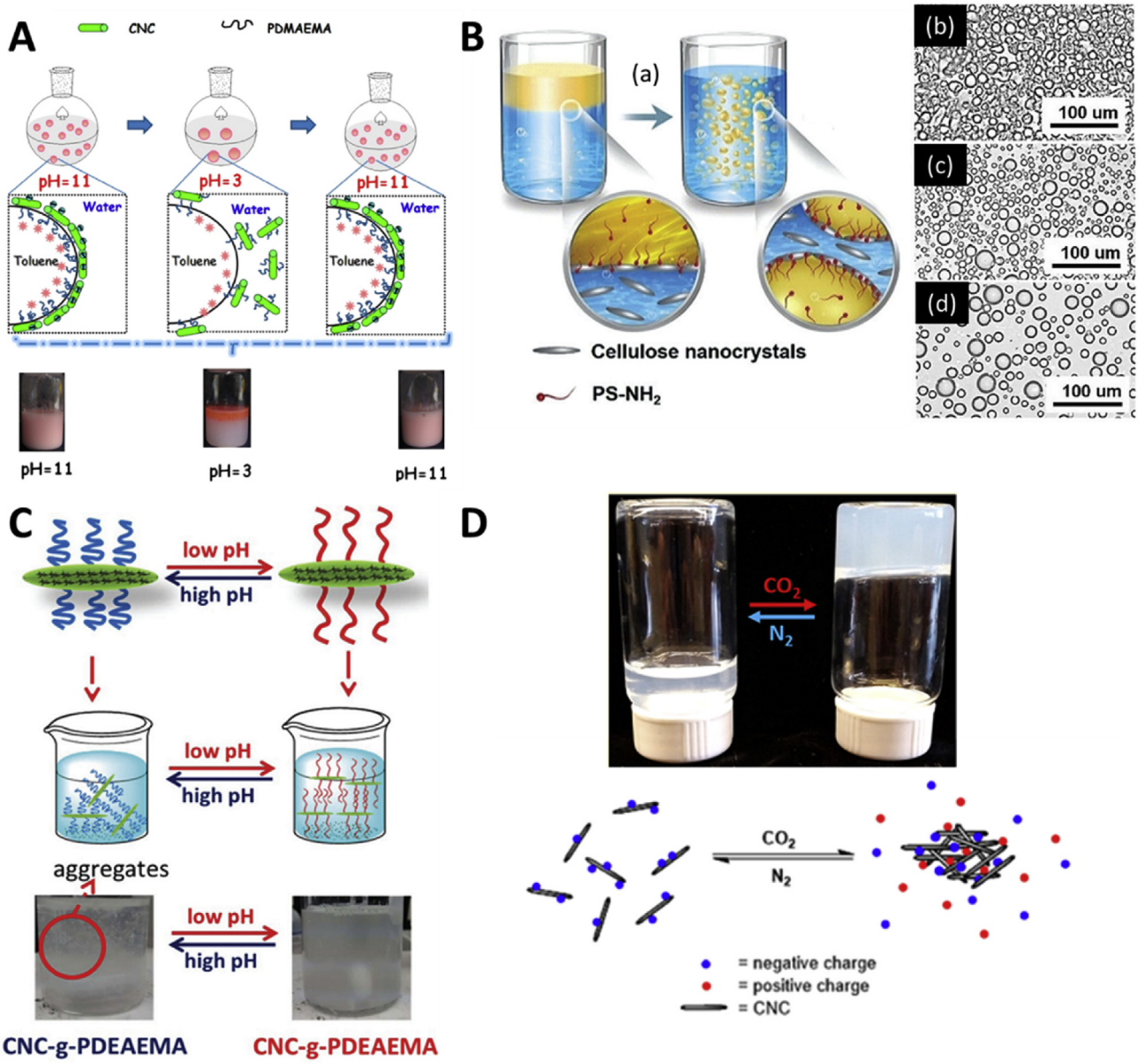

Fig. 3. (A) pH-responsive behavior of toluene-in-water emulsion stabilized by CNC-g-PDMAEMA (5 wt%) by adjusting the pH values of the continuous phase [58]. (B) Illustration of formulation of CNC-based Pickering emulsions (a) and Optical micrographs of Pickering emulsion droplets stabilized by CNCs at different pH values, (b) pH 3.0, (c) pH 5.0, and (d) pH 7.0 [56]. (C) Schematic of CNC-g-PDEAEMA dispersion in water at high pH and low pH [5]. (D) Reversible aggregation and dispersion of the CO_2-switchable CNC suspensions containing imidazole in the presence and absence of CO_2 [53].

required a certain grafting density and length of the grafted polymer chains. Eyley et al. [62] reported on an imidazole-grafted CNC which were evaluated for the pH-responsive flocculation of a green microalgae called *Chlorella vulgaris*. The surface-functionalized CNCs exhibited positive surface charge at low pH and negative surface charge above pH 7, which were demonstrated in a CO_2-induced flocculation of microalgae with an efficiency of 200 mg L^{-1}. Chen et al. [63] reported on one kind of surface-functionalized CNC with both pH-responsiveness and fluorescent characteristics. By grafting poly(amidoamine) (PAMAM) to the surface of 2,2,6,6-tetramethyl-piperidinyl-1-oxyl radical (TEMPO)-oxidized CNCs (carboxylated CNC), the obtained CNC-PAMAM exhibited strong fluorescent emission, and the intensity of the emission was associated with aggregation with changes in the pH.

The application of pH-responsive CNC in biomedicine, such as drug release and drug delivery, has also attracted increasing attention in recent years. Rahimi et al. [64] reported on the tris(2-aminoethyl)amine-functionalized CNC decorated Fe_3O_4 biocompatible nanoparticles, which were designed for the delivery of methotrexate (MTX). MTX was loaded via the electrostatic attraction between positively charged amino groups on the CNC carrier and negatively charged carboxylate group on the MTX molecules at the physiological pH of 7.4. The controlled release of MTX was pH-responsive because of the protonation of carboxylate groups on MTX, which have the potential for use in targeted drug delivery in cancer treatment. Another pH-controlled CNC-based nanocomposites for drug release was reported by Li et al. [65]. Folate/cis-aconityl-doxorubicin@polyethylenimine@CNC (FA/CAD@PEI@CNC) nanomedicines were developed by designing a hierarchical pH-

controlled CNC-based nanocomposite for doxorubicin (DOX) loading. The drug released of DOX approached a maximum of 95% at pH 5.5, and a controlled release of 17% was achieved at pH 7.4.

pH-responsive CNC hybrid systems have also been proposed for use in imaging systems. Tang et al. [66] reported a pH-sensitive fluorescein-functionalized CNC, where a pH-indicator dye, 5 (and 6)-carboxy-2′,7′-dichloro-fluorescein (CDCF), was grafted onto CNC by applying L-leucine amino acid as a spacer linker. The pH-responsive character of the system was investigated, and it was found that the fluorescence intensity of the CNC compound increased with increasing pH, spanning a large pH range of between 2.28 and 10.84. Tam and co-workers synthesized CNC-based optical pH indicators using polyrhodamine (PR)-coated CNC. In-situ polymerization was used to deposit PR onto cellulose generating a compound that was both highly dispersible in aqueous systems and capable of changing color reversibly with pH [67].

pH-responsive CNCs have also been incorporated into switchable hydrogel nanocomposites. Way et al. [68], for example, reported on two kinds of surface-functionalized CNC that could switch from suspension to hydrogel in response to pH changes. Oechsle and coworkers [53] also reported a CO_2-switchable hydrogel that was prepared by mixing CNC suspension with imidazole. The gelation of CNC−imidazole suspension was induced by sparging CO_2 (shown in Fig. 3D), caused by the electrostatic attraction between CNC and protonated imidazole at low pH. This could be reversed simply by sparging with N_2, leading to the deprotonation of imidazole and the subsequent electrostatic repulsion between the components. Cha et al. [54] reported on hydrogels containing N-isopropyl acrylamide and carboxylated CNC. The prepared hydrogels exhibited swelling behavior in response to pH changes, due to varying charges on the CNC as the carboxylate groups became protonated and deprotonated.

2.3. Multi-responsive and miscellaneous adaptable systems

Although temperature and pH-sensitive polymer systems represent most of the recent research undertaken on smart CNC hybrid systems, some effort has also been devoted to prepare systems that respond to other types of stimuli. There are benefits to producing materials that respond to specific and less ubiquitous stimuli than temperature or pH, as these materials may be better suited for precision applications. CNC-based systems that respond to a range of stimuli including water, magnetic fields, strain, and combinations of stimuli like temperature and pH have been developed. Low and coworkers [69], for example, developed a drug delivery system based on magnetic Fe_3O_4 decorated CNCs. A colon cancer targeting drug, curcumin, was loaded into a Pickering emulsion stabilized by the magnetic CNCs. Following exposure to a magnetic field, the system was capable of releasing 53.30% of the loaded drug over a 4-day period. Nylepö et al. [70] also developed a magnetically active CNC system, decorating the surface of the cellulose with magnetic nickel/cobalt particles. A film of the CNC−Fe_3O_4 compound was formed by a simple solvent removal, and the film became rigid upon exposure to a magnetic field.

Water-responsive smart materials have also been prepared using CNC as a primary component. Wang et al. [71] incorporated CNCs into a mixture of graphene and carbon nanotubes, which was then embedded into an elastomeric matrix. The composite material was exposed to many types of water (hot vapor, room temperature mist, and a water droplet), and in all cases, the materials' electrical resistance increased dramatically within a matter of minutes. The notable change is suggested to be due to the infiltration of water into the composite, pushing the carbon-based conductive elements apart. Additionally, the authors proposed that the water diffusivity into the matrix was facilitated by the presence of the hydrophilic CNC. This composite has promising potentials in applications, such as flexible and responsive electronics or sensors.

CNCs were combined with electroactive polymers to generate smart materials that can bend in the presence of an applied electric field. Kim et al. [72] fabricated an electroactive actuator using poly(vinylidene fluoride)/CNC electrospun membranes and found that increasing the CNC concentration both increased the actuator's displacement and decreased the response lag time. These improvements were attributed to the increase in electrolyte holding capacity in the actuator system as a result of CNC incorporation. Ko et al. [73] prepared a transparent and flexible actuator based on a dielectric elastomer polyurethane. This polyurethane was produced using CNCs mixed with the polyol, poly[di(ethylene glycol) adipate] and hexamethylene diisocyanate as the necessary isocyanate salt. The authors found that at relatively low loading of CNC, up to 10% strain could be generated by applying a weak (3 V μm^{-1}) electric field. This smart system is promising for applications, such as tunable lenses, where low power consumption and transparency are critical.

CNCs have also been shown to improve the piezoelectric properties of electroactive polymers. Poly(vinylidene fluoride) (PVDF) is one of the most widely investigated piezoelectric polymer materials, and the presence of the β crystalline phase is the most important for piezoelectric performance [74]. It has been shown that the incorporation of CNC in PVDF can promote the formation of β crystalline phase, improving the piezoelectric performance [75,76]. In the future, this may allow for smart electroactive systems to be developed with high sensitivity to compression or strain.

Han and coworkers [77] developed a piezo-resistive smart system containing CNC, which could sense strain through reversible increase in resistance. To achieve this, a conductive PVA composite film with polypyrrole (PPy)-functionalized CNCs was developed [3]. The CNCs functioned as biotemplates, which enabled the uniform aqueous dispersion of insoluble PPy. The CNC-PPy particles were then mixed with PVA solution, cast, and dried to obtain PVA nanocomposite films. In a strain sensing experiment, the prepared CNC/PVA film could respond to strain from human motion through a highly sensitive change in resistance, and it could distinguish between different motions, such as swallowing and wrist bending.

In addition to single-stimulus responsive systems, multi-responsive CNC systems have also been investigated in recent years. Tang et al. [78] prepared CNCs with grafted binary polymer brushes, via cerium-mediated polymerization of thermo-responsive oligoethylene glycol methacrylate (OEGMA) followed by ammonium persulfate initiated polymerization of methacrylic acid (MAA) to achieve pH-responsiveness in an aqueous solution. An oil−water Pickering emulsion stabilized by the resulting CNC-g-POEGMA-PMAA nanoparticles could be destabilized by decreasing the pH or increasing the temperature. Upon heating the heptane-in-water emulsions stabilized by CNC-g-POEGMA-PMAA (0.3 wt %) to 70 °C (above LCST of POEGMA), nanoparticle aggregation occurred. The hydrogen bonding between polymer brushes was then controlled by external pH. At pH 2.0, strong hydrogen bonding formed between binary polymer chains inducing the coalescence of emulsion droplets. This change in intermolecular force switches the stability of the emulsion that can enhance oil−water separation. Due to the nanoparticle aggregation, the oil droplets became unstable, resulting in the coalescence of oil droplets into larger sizes.

Haqani et al. [79] designed a dual-responsive CNC-g-copolymer that can respond to the physiologically relevant pH and temperatures (5.0−7.4 and 37°C), making this material well suited for drug delivery applications. CNC was first coated with crosslinked poly(2-hydroxyethylmethacrylate) (PHEMA) to increase the content of hydroxyl groups at the surface for reaction with RAFT agent. s-(thiobenzoyl)thioglycolic acid was grafted to the surface of CNC-

Table 2
An overview of recent publications on smart chiral nematic CNC materials.

Response Stimulus	Chiral Film Formulation	Maximum Reflected Wavelength	Ref.
Chemoresponsive			
Humidity	3.8% glycerol/96.2% CNC (w/w)	586 nm at 16% RH, 704 nm at 98% RH	[87]
Humidity	20% polyethylene glycol/80% CNC (w/w)	~500 nm at 30% RH, ~900 nm at 100% RH	[88]
Humidity	Sodium chloride; NaCl/CNC ratio of 25 mmol/kg	~440 nm at 0% RH, ~750 nm at 100% RH	[85]
Water	54.5% polyethylene glycol diacrylate/45.5% CNC (w/w)	515 nm in dry state, 730 nm in wet state	[86]
Ethanol	30% waterborne polyurethane/70% CNC (w/w)	441 nm immersed in EtOH, 600 nm immersed in 40/60 EtOH/water soln	[89]
Mechanoresponsive			
Compression	100% desulfated CNC	None when uncompressed, 410 nm when compressed in wet state	[90]
Uniaxial Strain	Glucose/ethyl acrylate/2-hydroxyethyl acrylate/CNC	None; birefringence increases with increasing strain	[27]
Uniaxial Strain	Glucose/ethyl acrylate/2-hydroxyethyl acrylate/CNC	~490 nm when uncompressed, ~675 nm with 40% strain; birefringence decreased with increasing strain	[91]
Multiresponsive			
Uniaxial Strain, Humidity	30–50% glucose/70–50% CNC (w/w)	*Strain*: 730 nm at rest, 626 nm with 140% strain *Humidity*: ~400 nm at 10% RH, ~1000 nm at 100% RH	[84]
Compression, Ionic Strength	30% acrylamide/70% CNC (w/w)	*Compression*: 650 nm when uncompressed, 500 nm under 3.7 kPa load, 450 nm under 6.5 kPa load *Ionic Strength*: 620 nm in water, 475 nm in 1×10^{-3} M NaCl solution	[92]
Heat, Humidity	Poly(N-isopropylacrylamide)/glutaraldehyde/CNC	*Humidity:* 424 nm at 70% RH, 518 nm at 97% RH *Heat*: 424 nm at room temperature, 511 nm at 40 °C	[93]

PHEMA as the chain transfer agent. NIPAM and acrylic acid (AA) were then polymerized from the surface of CNC-PHEMA with different sequence to prepare CNC-PHEMA-g-PNIPAM-PAA and CNC-PHEMA-g-PAA-PNIPAM. When PAA was the outer block, LCST was shifted to near body temperature and pH-sensitivity was observed at pH values of 7.0–10.0.

Yuan et al. [80] synthesized CNC-g-P(AzoC6MA-co-DMAEMA) via the ATRP of AzoC6MA and 2-(N,N-dimethylamino)ethyl methacrylate (DMAEMA) monomers. The CNC platform promoted the dispersion of fluorescent sensors in aqueous solutions for potential in-situ detection and monitoring of temperature or pH in organisms or water. By increasing the temperature (over LCST of CNC-g-P(AzoC6MA-co-DMAEMA)) or increasing the pH (above p*Ka* of CNC-g-P(AzoC6MA-co-DMAEMA)), grafted brushes undergo conformational transitions. The collapsed conformation limits the *trans-cis-trans* transition of the azobenzene groups, and consequently, more stable *trans* conformations are likely to form under UV-irradiation, which leads to a significant increase in the fluorescence intensity.

Malho et al. [32] reported on the surface-functionalized CNCs engineered to possess both temperature and pH-responsive properties. Thermal-responsive biosynthetic elastin-like polypeptides (ELPs) and pH-sensitive PAA were grafted onto CNCs via the surface initiated atom transfer radical polymerization (SI-ATRP). The colloidal stability was controlled by changing the temperature and pH of the CNC dispersion, which has potentials for various biological applications.

3. Optically adaptable smart systems

Significant research has also been undertaken to develop optically adaptable smart materials. These are materials whose optical properties, such as reflectance or birefringence, change in response to an external environmental stimulus. CNCs, often thought of primarily in terms of their mechanical strength and easy surface manipulation, can also have high levels of optical activity. When CNCs were dispersed in a solvent at a sufficiently high concentration (above 8 or 8.5 wt%) and then allowed to self-assemble during solvent evaporation, they formed chiral nematic films [81,82]. The CNC chiral nematic films are always lefthanded, allowing them to reflect lefthanded circularly polarized light with a distinct maximum wavelength. The peak wavelength from the reflection of the films is dependent on the pitch of the cellulose films, which is defined as the total distance it takes for the chiral structure to make a full turn. The pitch of CNC films can be manipulated relatively easily without destroying the chiral nematic structure through the infiltration of small molecules, solvents, and polymeric materials into the gaps between each chiral layer [83,84]. In turn, the maximum reflected wavelength, and thus the perceived color, can be easily tuned. More interestingly, the pitch change in CNC photonic films can be reversed, for example, through the addition and subsequent evaporation of water molecules. This fact makes CNC chiral films prime candidates for optically adaptable smart materials.

Much research has been carried out recently on the use of smart, optically changeable CNC films, with applications ranging from security and anticounterfeiting to sensors [85,86]. An overview of the most recent research in this area is summarized in Table 2. A vast majority of this recent work has been focused on CNC films that change color (as in, whose peak reflected wavelength shifts), and the work can be divided into two primary categories: materials that change color in response to applied mechanical stress and materials that change color in response to a change in relative humidity. Additionally, there are a variety of different techniques that have been explored to provide the materials with fast and reproducible color change, as well as to incorporate desirable mechanical properties to the final material.

3.1. Mechano-responsive photonic systems

A broad range of mechano-responsive photonic CNC materials have been developed in the past several years, including aerogels, hydrogels, and composite films [27,84,90,92]. Cao et al. [90], for example, developed a pressure-responsive aerogel using a combination of evaporation-induced self-assembly and ice templating. The ice templating was proposed to reduce the pitch of the chiral structure from multiple micrometers to the nanometer range, allowing for the reflection of visible light. In uncompressed form, the aerogel is white and opaque, indicating that the light is primarily being scattered. However, upon compression of the aerogel, especially when saturated with water or other solvents, the 3D structure collapses to a 2D chiral structure, and Bragg reflections

prevail. This allows the gel to change from broadband scattering to distinct reflection and back with changes in pressure, lending the aerogel with this unique mechano-responsive property.

Hiratani et al. [92] have also proposed novel fabrication methods for pressure-responsive CNC photonic systems, using a composite of CNC and polymerized acrylamide to form a photonic hydrogel. A shear alignment process, in which the hydrogel was subjected to alternating shear along one axis prior to polymerization, allowing for the creation of highly anisotropic films as shown in Fig. 4A(a). A long range and an anisotropic order are clearly visible in the sheared sample but not in the unsheared sample (Fig. 4A(b)). The sheared photonic composite also shows remarkable pressure responsiveness, drastically changing color at pressures as low as 1.4 kPa. The color progression showed a blue shift as the pressure was increased corresponding to a decrease in the chiral pitch as shown in Fig. 4A(c). The unusual progression from green to blue to red could be explained by two separated reflectance peaks — one that moves from the green and blue region quickly to the UV region upon compression, and another that moves from the IR region into the red visible light. The developed CNC−polyacrylamide hydrogel possessed a good and cyclable pressure responsiveness and could easily be applied as an optical pressure sensor.

When not incorporated into a gel, the CNC photonic films formed during the evaporation-induced self-assembly was quite brittle, with relatively high ultimate strengths and relatively low elongation to break. Qu et al. [84] sought to prepare mechano-responsive photonic films with improved mechanical properties by introducing glucose units to the CNC solution prior to self-assembly, which could then act as plasticizers by forming a percolating network of hydrogen bonding throughout the layers of chiral sheets. By varying the ratio of CNC to glucose from 100/0 through 50/50, the elongation at break increased to a strain of 40%, compared to the initial 1.7% strain of the CNC film alone. Additionally, the films produced with varying glucose content had different maximum reflectance, and increasing the glucose content led to an increase in the maximum reflectance (red shift), which is indicative of the glucose molecules intercalating within the CNC chiral structure that increases the pitch. In response to uniaxial tensioning, the 50/50 CNC/glucose film displayed a reversible blue shift in optical reflectance, which is attributed to the reorientation of some of the CNC layers from chiral nematic to nematic.

Kose et al. [27] prepared a CNC and elastomer composite that responds to strain viachanges in the nematic structure rather than the pitch. CNC and glucose units were first combined and dried to form self-assembled chiral nematic structures, and the films were then swollen with DMSO to allow the infiltration of ethyl acrylate and 2-hydroxylethyl acrylate monomers. Following the polymerization, a completely transparent CNC elastomer composite was formed. Fig. 4B(a) shows the proposed mechanism by which the chiral nematic structure unwinds to a pseudo-nematic structure under uniaxial loading. This unwinding induces a drastic shift in the apparent color when viewed under a cross-polarizing lens. The distinct progression of color does not align with a blue or red shift, but rather with the Michel-Lévy color progression in response to the increased birefringence [94]. This confirms the supposition that the color change in the film is not due to a change in chiral pitch, but rather a reorientation of the CNC layers. In a further work, the same group prepared a shear-ordered version of their CNC−elastomer composite and explored its optical properties in response to uniaxial strain [91]. They found that when the elastomer was stretched parallel to the axis aligning the CNCs, there was a small increase in birefringence. In contrast, when the composite was stretched in a perpendicular direction (disordering the CNCs), the birefringence decreased drastically with increasing strain. This again emphasized the importance of the ‘unwound’ pseudo-nematic CNC structure in generating high levels of birefringence. In addition to distinct color change in response to stretching, the CNC−elastomer composites can withstand up to 900% strain, making them well suited for applications with high mechanical loading demands.

3.2. Humidity-responsive photonic systems

CNC chiral nematic films are also attractive humidity-responsive materials for applications such as humidity sensors, displays, or decorative coatings [87,89]. As discussed earlier, many of the humidity-responsive materials change color due to changes in the chiral pitch of the film as a result of water molecules infiltrating each nematic layer. One challenge in fabricating humidity-responsive CNC systems is finding a secondary material that can confer better flexibility or elasticity without impeding the diffusion of water molecules into the chiral nematic film. A simple solution is to incorporate a small hygroscopic molecule that can also act as a plasticizer. He et al. [87] achieved this by using CNC chiral nematic films impregnated with glycerol. Varying amounts of glycerol (0.2−1 g) were added to a 20 g suspension of 8.5 wt% CNC, and the mixture was allowed to self-assemble by evaporation. The pitch increased proportionally to the increasing glycerol content, thus red-shifting the maximum reflected wavelength from under 400 nm (no glycerol) to almost 650 nm (1 g of glycerol). The maximum elongation to break of the composite was achieved with the addition of 0.8 g of glycerol, which tolerated 4% strain before break. This sample was further investigated for its humidity response, with cycling between 16% and 98% relative humidity (RH). The color of the 0.8 g glycerol/CNC composite film changed from its native green at 16% RH to orange at 98% RH. The proposed relationship between water intercalation and color change is shown in Fig. 4C. To confirm the pitch expansion, they also tracked the thickness of the cast film, where it increased from 91 to 151 μm as humidity increased from 16% to 98%. This corroborates the hypothesis that the swelling of the CNC film through water molecule infiltration is the primary driver for the color change.

Yao et al. [88] have attempted to overcome the limitations of neat CNC films through the addition of polyethylene glycol (PEG), which may even improve the speed and magnitude of water intercalation due to its high hydrophilicity. Through a simple mixing of PEG and CNC and then drop casting, CNC/PEG composites were formed ranging from a 100/0 to a 60/40 weight ratio. As expected, the incorporation of a polymer generated a progressive red shift in the base color of the composite, as seen in Fig. 4D(a). Increasing PEG content increased the maximum elongation at break to about 2.5%, double of what was observed in neat CNC films. Upon exposure to the changing relative humidity, the CNC/PEG composite film changed from green to transparent, as shown in Fig. 4D(b). This change, which occurs on the order of seconds, is also reversible and cyclable.

Despite the challenges, it is possible to use neat CNC to achieve a final product that is flexible and responsive. The advantage of using neat CNC in such a case is that the fabrication process is significantly simplified, requiring only CNC suspended in a solvent above the concentration threshold necessary to form chiral nematic structures. Printing of humidity-responsive CNC films onto pre-patterned glass slides has been proposed by Zhao et al. [85] which allows for the generation of scalable arrays. Small circular CNC films, with diameters of 1000 μm and thicknesses of less than 5 μm, were printed onto glass substrates using three main steps: micro-printing areas of high and low hydrophilicity on the glass, dropping CNC dispersions onto the hydrophilic locations, and then covering the glass with immiscible hexadecane oil to allow for slower and controlled water evaporation. Because of the independence and

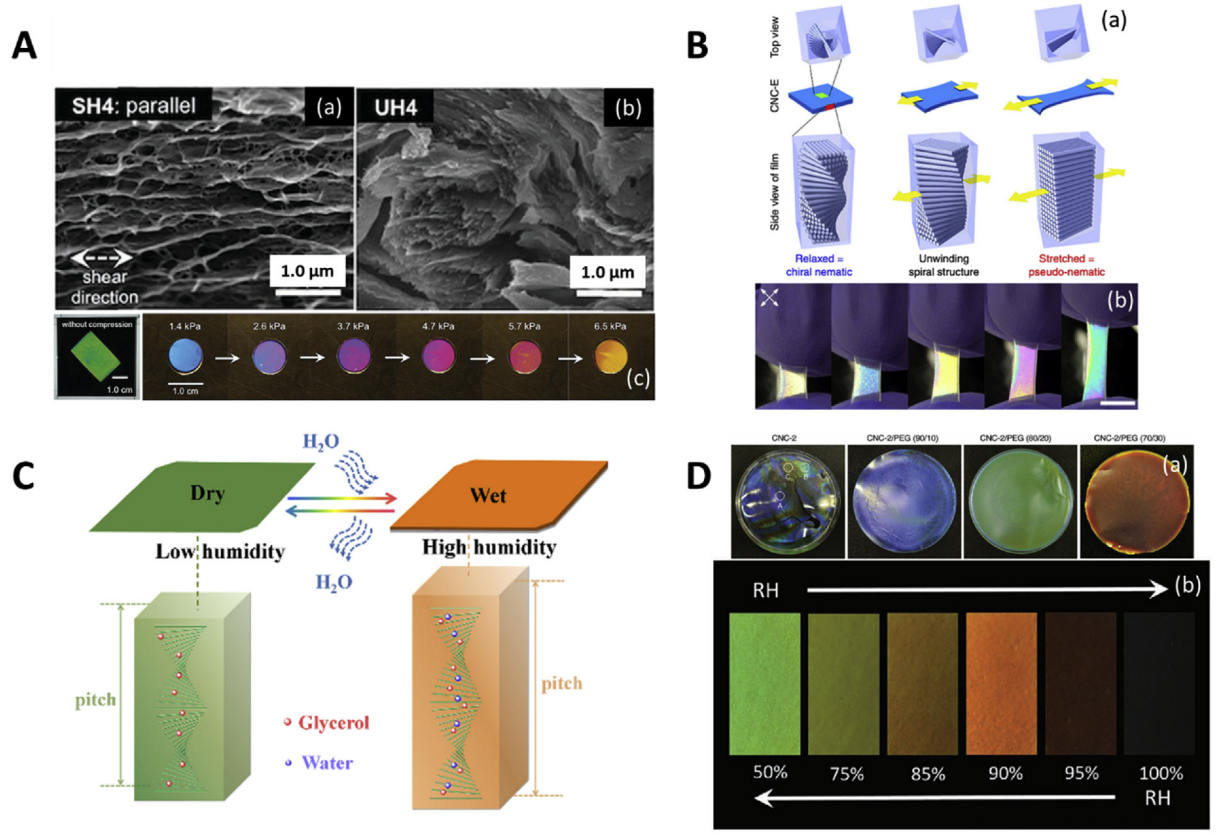

Fig. 4. (A) SEM images of shear-ordered anisotropic CNC films (a) and non-sheared CNC films (b); (c) the color of shear-ordered CNC films in response to changing pressure, as seen through cross-polarized lenses [92]. (B) Mechanism by which chiral nematic structure unwinds in response to applied mechanical stress (a). CNC–elastomer composite viewed with cross-polarizing lens, where scale bar represents 1 cm. (b) [27]. (C) Proposed mechanism for increase in chiral pitch and subsequent increase in maximum reflected wavelength [87]. (D) CNC/PEG composite films ranging from 100/0 to 70/30 weight ratios (a), 80/20 CNC/PEG composite's visible color change upon change in relative humidity from 50% to 100% and back (b).

dimension of each small CNC dot, a larger pattern can be printed on a flexible substrate without the cracking of the individual films. Each dot can also absorb a large amount of water in a matter of seconds, allowing for the rapid color change in response to changes in RH, such as breathing. The relatively large surface area to volume ratio of the CNC films also allows for shrinking to occur quickly when the humidity is lowered.

4. Self-healable nanocomposites

Crack formation and propagation in polymeric materials may lead to a dramatic loss in their load-carrying capacity, limiting their safety, reliability, durability, and lifetime. Producing materials that can repair themselves autonomously or upon exposure to an external stimulus can address this problem and improve the functionality and lifespan of the polymer [95–97]. Two major strategies have been employed to produce self-healing polymeric materials. The first strategy is based on dynamic noncovalent interactions, such as host–guest interactions [98], hydrogen bonds [99,100], metal ion co-ordinations [95,101,102], π–π interactions [55], and electrostatic interactions [97,103]. The other major strategy is to rely on reversible dynamic covalent bonds, such as β-hydroxyl ester bonds [104], boron–oxygen bonds [105] (phenylboronate ester), sulfur–sulfur bonds (disulfide) [106], carbon–nitrogen bonds (imine [107], enamine [108], and acylhydrazone [96]), carbon–carbon/carbon–sulfur bonds [109] (reversible radical reaction), and cyclohexenes (reversible Diels–Alder cycloaddition [110]). One of the most important challenges in designing self-healable materials is the seemingly conflicting need for both high stiffness, necessary for practical application, and high molecular dynamics, which form the basis of the healing process [98,105]. Adding CNC may address this problem by enhancing the stiffness of the composites with minimal disruption of the molecular dynamics. CNC can be used either as a reinforcer or as an active component in the structure of self-healable nanocomposites. When CNC was used as an active cross-linker, the high number of available surface functional groups could contribute to the reversible non-covalent or covalent bonds, promoting the self-healing efficiency [95]. CNCs are most often incorporated into self-healable hydrogels [96,98,105] and elastomers [99,104].

4.1. Self-healable nanocomposites based on dynamic noncovalent interactions

Modified and unmodified CNCs have been widely adapted in self-healable nanocomposites based on dynamic non-covalent interactions because of their high specific surface area and aspect ratio, as well as high mechanical strength and stiffness. The abundance of available surface hydroxyl groups promotes hydrogen bonding, whereas facile surface functionalization could be exploited to introduce hydrophobic interactions, electrostatic interactions, or π–π stacking into the system.

Coulibaly et al. [95] reported on the preparation of a healable metallo-supramolecular polymer (MSP) assembled from a telechelic poly(ethylene-co-butylene) that was end-functionalized with 2,6-bis(1′-methylbenzimidazolyl) pyridine (Mebip) ligands

and $Zn(NTf_2)_2$. Their investigations revealed that binding CNCs with Zn^{2+} ions induced the assembly of the MSP. Healing was achieved upon the absorption of incident ultraviolet (UV) radiation and its conversion to heat, which causes the dissociation of the metal–ligand motifs. The removal of UV light allows for the reassembly of MSP, and the original properties are restored, as shown in Fig. 5A. When the molar ratio of Zn^{2+} to functionalize poly(ethylene-co-butylene) was 1, the healing efficiency of a damaged sample (cut to a depth of~50–70%) exposed to a light with wavelength of 320–390 nm and a power density of 350 mW/cm^2 was found to be 100%. The healing efficiency was determined by comparing the toughness values taken before the damage and after healing.

Liu et al. [102] prepared conductive, elastic, self-healing, and strain-sensitive hydrogels from a soft cross-linked network of poly(vinyl alcohol) (PVA) and poly(vinylpyrrolidone) (PVP) and a hard network of sacrificial CNC–Fe^{3+} coordination bonds. The soft network transfers the tension to the reversible sacrificial CNC–Fe^{3+} coordinates. The reorganization of CNCs and Fe^{3+} via ionic coordination is the mechanism of self-healing. They evaluated the self-healing performance by measuring the conductivity of the self-healed material. Zhu et al. [97] produced a hydrogel by mixing poly(vinyl alcohol) (PVA) and a series of ionic liquids including methylimidazolium hydrogen sulfate ($BmimHSO_4$). In order to improve the mechanical properties and self-healing performance, they polymerized a network of polyacrylamide-co-polyacrylic acid (PAM-co-PAP) via free radical polymerization. They also introduced graphene oxide (GO) and CNC to their structure to improve the mechanical properties. Due to the ionic bonds between the cations of ionic liquid and the hydroxyl groups of PVA, a healing efficiency of 93.8% (based on tensile strength) was achieved after 24 h of healing in air without any external stimulus. Cao et al. [99] sought to increase the self-healing capability of epoxidized natural rubber (ENR) by adding CNC. Introducing dynamic hydrogen bonding between oxygen-containing groups of ENR and hydroxyl groups on the CNC surfaces resulted in slightly cross-linked rubber chains, which improved the self-healing and mechanical properties. Additionally, the healing efficiency increased with increasing CNC content. The healing efficiency (estimated from toughness calculated from the area under the stress–strain curves) of ENR comprising 20 wt% CNC could approach 86% after 24 h of healing at room temperature. In another work by Fox et al. [55], π-electron rich pyrenyl end-capped oligomer and a chain-folding oligomer containing pairs of π-electron poor naphthalene-diimide (NDI) units were mixed to form a supramolecular polymer blend via π–π interactions. The effect of CNC on the mechanical and healing properties was elucidated, and the best results were obtained for the nanocomposite comprising 7.5 wt% CNC, where a 20-fold increase of tensile modulus was achieved along with full healing at 85 °C within 30 min.

Bai and coworkers [103] prepared a self-healing composite by grafting 4-vinylpyridine (4VP) from the surface of CNC via metal-free photoinduced electron transfer atom transfer radical polymerization (PET-ATRP). Free radical polymerization of AA in the presence of CNC-g-P4VP was then performed to produce the final composite. Non-covalent dynamic electrostatic interactions between protonated pyridine groups of P4VP and deprotonated carboxylic acid groups of PAA formed the basis of the self-healing behavior. The incorporation of about 0.1 wt% of CNC-g-P4VP into the PAA resulted in a material with 85.9% self-healing after 6 h.

Shao et al. [101] prepared a tough, self-healing, and self-adhesive hydrogel from cross-linked PAA, tannic acid-coated CNCs (TA@CNC), and Al^{3+} ions. After coating CNCs with tannic acid, free radical polymerization was used to polymerize and crosslink the AA. In order to produce metal–phenolic coordination between TA@CNCs, metal–carboxylate coordination between PAA chains, and hybrid coordination between TA@CNCs and PAA chains, composite gels were immersed into the $AlCl_3$ solution. This produced multiple, dynamic coordination bonds and provided the hydrogel with reliable mechanical and electrical self-healing properties. More than 90% healing efficiency was achieved for hydrogels containing more than 0.8 wt% of tannic acid-coated CNCs, following a 30 min healing period at room temperature. McKee and coworkers [98] also prepared a nanocomposite hydrogel, by combining a polymer brush grafted CNC and methyl viologen-functionalized poly(vinyl alcohol) bound together by cucurbit [8]uril (CB[8]) supramolecular crosslinks. A random copolymer of dimethylaminoethyl methacrylate (DMAEMA) and naphthyl-functionalized methacrylate (NpMA) repeating units was grafted from the CNC surface by SI-ATRP. Methyl viologen and naphthyl units of grafted brushes interacted via dynamic host–guest interactions, allowing for the rapid hydrogel recovery from the sol-state. A schematic of this host–guest interaction is shown in Fig. 5C. The resulting hydrogel achieved rapid recovery giving rise to a high storage modulus due to the specificity of the three-component host–guest interactions. This dynamic system also allowed for self-healing to occur even between surfaces that had been exposed to ambient conditions, which is a challenge many self-healing systems still face.

Biyani et al. [100] functionalized both telechelic poly(ethylene-co-butylene) chain ends and the surface of CNCs with hydrogen-bonding ureidopyrimidone (UPy) groups. By mixing these two components, they were able to generate a light-healable nanocomposite. Nanocomposites comprising 15 and 20 wt% of CNC–UPy showed 100% healing efficiency (based on tensile strength) after being healed by exposure to light of a wavelength of 320–390 nm and an intensity of 250 mW/cm^2 for 80 s. In comparison, the composite without CNC could only achieve a healing efficiency of 81% under similar conditions.

4.2. Self-healable nanocomposites based on dynamic covalent interactions

Huang et al. [107] fabricated an injectable self-healing nanocomposite hydrogel by mixing carboxymethyl chitosan (CMC) and dialdehyde-modified CNC (DACNC) for potential wound dressing applications. DACNCs prepared by periodate oxidation of CNC act as both crosslinker and reinforcer of the hydrogel. The amine groups of CMC can react with aldehyde groups of DACNC to form dynamic and reversible Schiff-base linkages, which can be readily broken and re-formed, yielding a self-healing system. By integrating the above self-healing with elastic polyacrylamide (PAAm) network, they also prepared a stretchable, tough, and self-recoverable hydrogel for applications in load-bearing tissues, such as artificial cartilage and muscle tissue [111]. In another study, Liu and coworkers [108] produced a hydrogel from cellulose acetoacetate (CAA), hydroxypropyl chitosan (HPCS), and amino-modified CNCs (CNC–NH_2). The hydrogel was assembled through the formation of dynamic covalent enamine bonds between the amino groups of chitosan, and the CNC–NH_2 and acetoacetyl groups of CAA, along with hydrogen bonding of the three components. The mechanism of self-healing relies on the dynamic nature of the enamine bonds at low pH. Shao et al. [110] fabricated a self-healing hydrogel from flexible polymer chains of dimaleimide poly(ethylene glycol) (Mal-PEG-Mal) crosslinked with furyl-modified CNCs through thermally reversible covalent Diels–Alder click reaction. Diels–Alder linkages formed by a conjugated diene and a dienophile can be cleaved on heating to achieve a new equilibrium, resulting in the healing of the hydrogel. A healing efficiency (based on tensile strength) of 78%

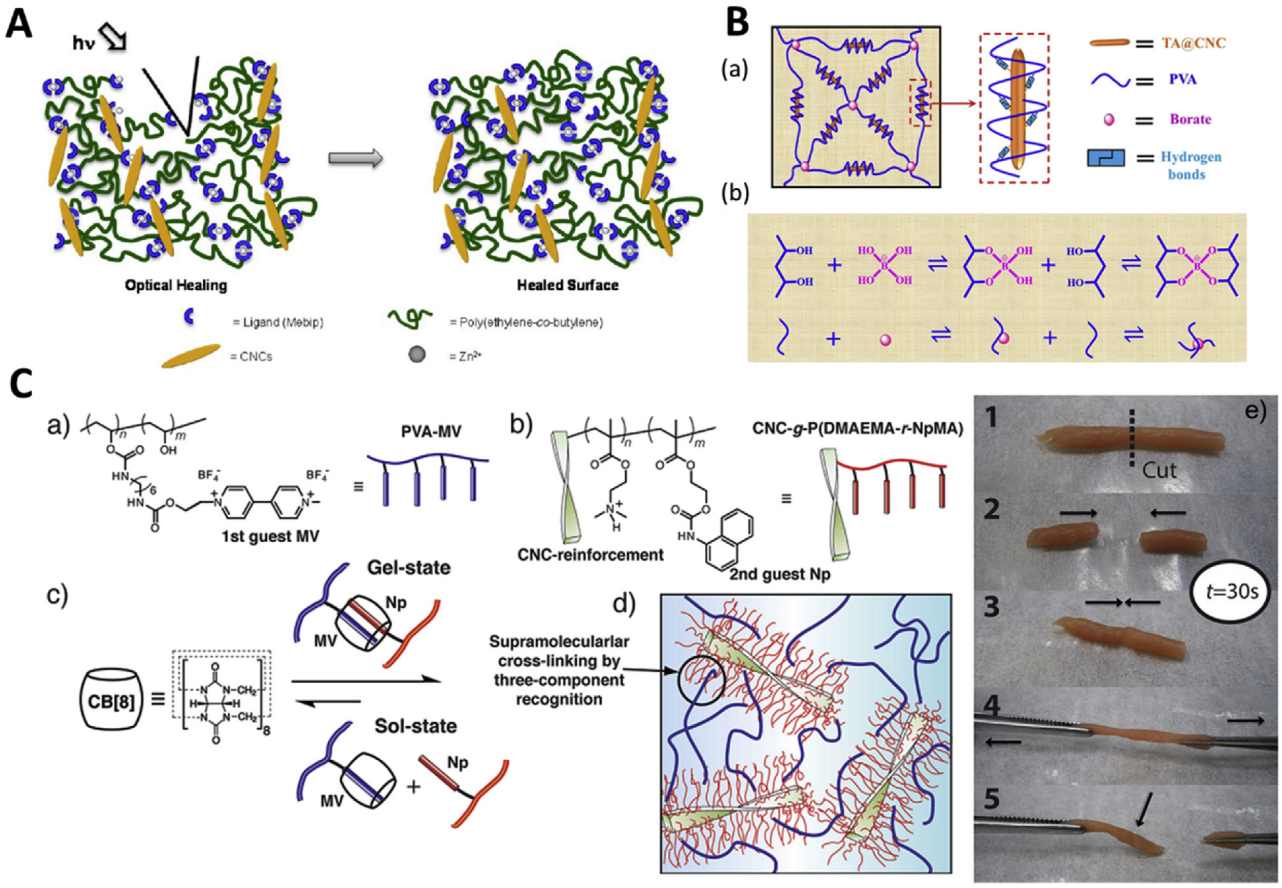

Fig. 5. (A) Schematic representation of the metallo-supramolecular nanocomposites and healing mechanism [95]. (B) Schematic illustration of the self-healing gel networks with TA@CNC and PVA-borate (a). Reversible borate-diol complexation between PVA and borax (b) [105]. (C) Schematics and architecture for three-component supramolecular hydrogels based on CNC and CB [8] host–guest chemistry. (a) PVA containing the first-guest methyl viologen functionality (PVA-MV). (b) CNCs containing copolymer grafts of protonated dimethylaminoethyl methacrylate (DMAEMA) and second-guest naphthyl methacrylate (NpMA) repeat units (CNC-g-P(DMAEMA-co-NpMA)). (c) CB [8] as the host motif. (d) Selective supramolecular cross-links based on three-component recognition by CB [8] binding together the components into dynamic hydrogels where the modified PVA bridges the CNC-grafts together. (e) Qualitative demonstration of the self-healing of hydrogel [98].

was reported after 24 h of healing at 90°C for a hydrogel with a molar ratio of furyl to maleimide of 1:1.

Imato et al. [109] introduced diarylbibenzofuranone (DABBF)-based dynamic covalent mechanophores onto both poly(propylene glycol) (PPG) and the surface of CNC, and DABBF could be reversibly dissociated to two radicals. Because equilibrium conditions cannot persist with high concentrations of radicals, the radicals spontaneously recombine, which provides the basis of the composite's self-healing behavior. Xiao et al. [96] combined dialdehyde CNC (DICNC) with acylhydrazine-terminated polyethylene glycol to produce a biocompatible self-healing hydrogel through the formation of dynamic reversible acylhydrazone bonds, for potential tissue and biomedical engineering application. Dynamic reversible exchange of acylhydrazone bonds under acidic conditions allows for autonomous self-healing. For a hydrogel containing just 2.3 wt% DICNC, a 97.5% self-healing efficiency could be achieved after a 48 h healing period at a pH of 2.5. Li and coworkers [106] combined CNC, thiuram disulfide (TDS), triethanolamine (TEA), and hexamethylene diisocyanate (HDI) to prepare a self-healing gel by reshuffling the thiuram disulfide bonds to induce self-healing of the network. The healing efficiency of 97.3% (based on tensile strength) was observed for a gel containing 2.2 wt% CNC after exposure to visible light for 2 min. Cao et al. [104] fabricated a self-healable cross-linked rubber network by mixing TEMPO-oxidized CNC (TOCNC) and epoxidized natural rubber (ENR) through exchangeable β-hydroxyl ester bonds between TOCNC and ENR. Dynamic reshuffling of β-hydroxyl ester bonds via transesterification reactions at elevated temperature impart healing properties to this cross-lined network. They reported 80% self-healing efficiency (based on tensile strength) for a sample comprising 20 wt% of TOCNC healing at 160°C for 3 h. Shao et al. [105] prepared a hydrogel by incorporation of rigid tannic acid-coated CNC (TA@CNC) into poly(vinyl alcohol) (PVA)-borax dynamic networks. The synergistic interactions between borate-diol bonds and hydrogen bonds impart a typical self-healing behavior to the gels, as shown in Fig. 5B. They reported a healing efficiency of 92% (based on tensile strength) in the gel comprising 3 wt% of TA@CNC after healing for just 60 s.

5. Cellulose nanocrystals in shape memory systems

Shape memory polymers (SMPs) are a class of polymers that can switch from a temporary-induced shape to a permanent historical shape in response to one or more external stimuli. They have garnered attention for their tunable mechanical properties, wide range of applications, and relatively low cost [112,113]. To endow SMPs with the capability to switch between shapes, the materials are first fabricated in their permanent shape, and then subjected to a 'programming' phase where they are molded into the temporary shape through mechanical deformation or loading. Following programming, the material will stay fixed in the temporary shape until it is exposed to a certain stimulus, such as temperature, light, or pH,

which triggers its change back to a permanent conformation [114,115].

Shape memory polymers have been developed to respond to a large range of stimuli, and the basis of shape memory behavior is largely the same across all SMPs. The material is composed of a network containing net points (or hard segments) and switches (or soft segments) [114]. The net points, which can be either chemical or physical bonds, are what dictate the SMP's permanent shape. Ideally, these bonds do not change regardless of the stimulus or stress being applied to the material. The switches, as the name suggests, contain bonds that can form or dissipate in response to some external stimulus, and this malleability allows them to fixate the polymer into another temporary shape.

Shape fixity, R_f, and shape recovery, R_r, are two metrics by which shape memory behavior is most often evaluated. The equations describing the two properties are described below [116]:

$$R_f = \frac{\varepsilon_u}{\varepsilon_m} \times 100\% \quad (1)$$

$$R_r = \frac{\varepsilon_m(N) - \varepsilon_f(N)}{\varepsilon_m(N) - \varepsilon_f(N-1)} \times 100\% \quad (2)$$

where ε_u is the actual strain after unloading the material during the programming step, ε_m is the maximum strain achieved before unloading, and ε_f is the residual strain of the sample after the recovery step (not applicable for the first cycle).

Many SMPs, while having good flexibility or elongation properties, suffer from the inability to store significant amounts of strain energy (characterized by low fixity), or from low maximum stresses. In order to address these issues, there has been a growing interest in blending SMPs with fillers to generate composite materials [112]. CNCs, known for their easily modified surfaces and their high mechanical strength and stiffness, are particularly promising in this application. A summary of the shape memory polymer and CNC blends is documented in Table 3.

Recent advances in shape memory polymers that utilize CNC as a filler can be divided into two broad categories: those that use CNC as the switchable domain and those that use CNC as an additive to modulate some other property of a preexisting shape memory polymer. When CNC is used as a primary switchable phase, it often carries modifications on its surface that dictate its interaction with itself and any other phase present in the material. For example, the CNC surface may be modified with pyridine moieties that can participate in physical crosslinking only when deprotonated at pH values greater than 5. After the incorporation of the pyridine-containing CNC into a polymer matrix, the final composite is capable to retain its temporary shape or relax to the permanent one in response to a change in environmental pH [131]. Modified CNCs have also been used to endow the polymer composites with light-activated shape memory. Biyani et al. [129] decorated the surface of CNC with a benzophenone derivative (Bp-CNC) that can consume a hydrogen bond and produce a carbon−carbon bond upon exposure to UV light. Bp-CNCs were then incorporated into ethylene oxide/epichlorohydrin copolymer (EO-EPI) matrix, where they could be induced to form new bonds when exposed to UV light, as summarized in Fig. 6A.

CNC-based materials that can be used with or without separate polymer matrices, such as CNC grafted with soybean oil derivatives, have also been explored for use as shape memory materials [123,124]. In these works, soybean oil was grafted from the surface of CNC using ATRP, and secondary amine groups in the plant oil polymers readily participated in hydrogen bonding. The grafted CNCs are thermally responsive, as the hydrogen bonding will degrade at higher temperatures (80 °C and above), allowing the film to be manipulated into a temporary shape. At cooler temperatures, the hydrogen bonds reform to fix the material. Upon heating a second time, the reformed hydrogen bonds once again dissipate, allowing the material to relax to its original permanent shape.

While the easily modifiable surface of CNCs makes them attractive for use as switches in SMPs, they have also been explored for their use in improving other aspects of shape memory polymers, such as mechanical strength or shape fixity [119,132]. The simple incorporation of unmodified CNC into a shape memory polymer via blending or mixing prior to casting can greatly enhance the mechanical properties. Saralegi et al. [122] found that the incorporation of 2 wt% of CNC into a polyurethane increased the Young's modulus of the final material from 238 to 328 MPa, and Wu et al. [127] found that incorporating up to 25 wt% of CNC into a poly(-glycerol sebacate urethane) increased the Young's modulus of the final material by 44 times of its neat value of 1.09 MPa. By varying the amounts of CNC added to the polymer, Wu et al. further concluded that the vast improvement in mechanical properties was due to the percolation of CNC within the polymer, as demonstrated in Fig. 6B(a). It was demonstrated that even at the highest levels of incorporated CNC, the composite maintained its inherent water-activated shape memory behaviors, as shown in Fig. 6B(b,c,d).

The addition of CNC into SMPs has also been shown to improve not only the strength of the material, but the fixity. Nicharat et al. [117] incorporated phosphoric acid-derived CNC into a commercially available polyurethane via melt mixing. Although the use of phosphoric acid-derived CNC (as opposed to traditional sulfuric acid-derived CNC) was initially investigated to increase the thermal stability of the CNC and allow them to withstand a melt mixing

Table 3
Recent examples of CNC/polymeric shape memory systems.

Switch Stimulus	Base Polymer(s)	CNC Modification	Ref.
Temperature	Poly(mannitol sebacate)		[116]
Temperature	Poly(tetramethylene glycol)	Functionalized with phosphorous groups	[117]
Temperature	Polycaprolactone		[118]
Temperature	Polycaprolactone and polylactic acid	PLLA or PCL grafted to surface	[119]
Temperature	Polylactic acid:polycaprolactone:polylactic acid	PLLA grafted to surface	[120]
Temperature	Polyurethane block copolymer		[121,122]
Temperature	Poly(soybean amide methacrylate)	PSBAM grafted to surface	[123]
Temperature	Epoxy soybean amide methacrylate and soybean amide methacrylate copolymer	ESBAM grafted to surface	[124]
Temperature	Hydroxyl-dominant poly(dodecanediol-co-citrate)	CNC arranged as chiral nematic flakes	[125]
Water/Temperature	Polyethylene glycol and polycaprolactone		[126]
Water	Poly(glycerol sebacate urethane)		[127]
Water	Polylactic acid	Carboxylmethyl cellulose sodium	[128]
IR Radiation	Epoxy oxide/epichlorohydrin copolymer	Functionalized with benzophenone derivatives	[129]
IR Radiation	Polycaprolactone and E12	Silver nanoparticles grafted/adsorbed to surface	[130]
pH	Polyethylene glycol and polycaprolactone	Functionalized with pyridine moieties	[131]

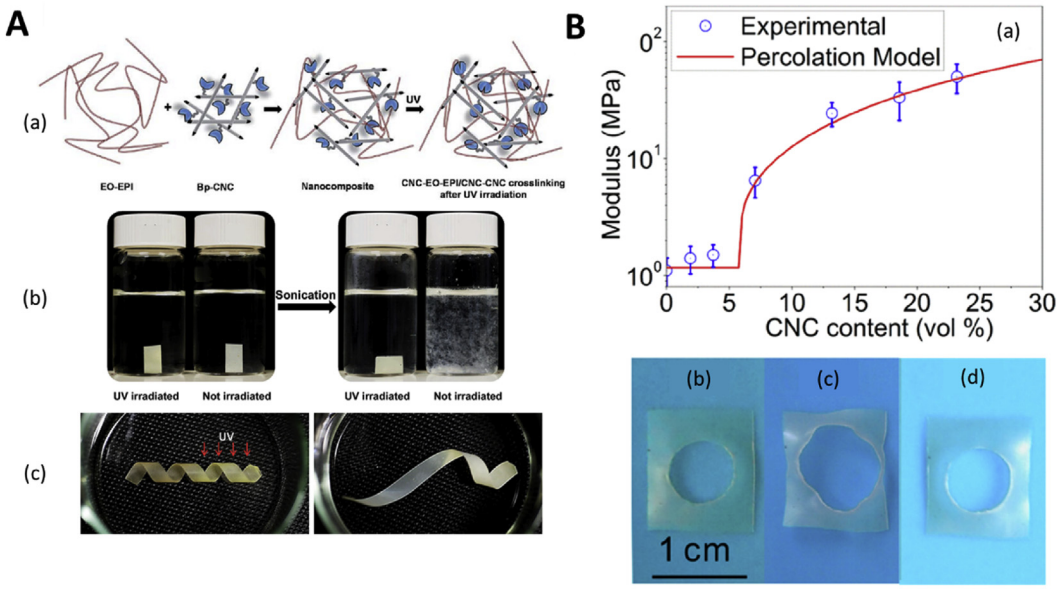

Fig. 6. (A) Schematic of preparation of EO-EPI/Bp-CNC nanocomposites and change in the architecture before and after UV exposure (a). Pictures of Bp-CNC films after just placing them in deionized water (left hand side) and after sonication for 30 min (right hand side). Prior to the experiment, one of the samples was exposed to UV (b). Pictures of the EO-EPI/Bp-CNC, showing the shape memory and light-activated shape fixing capabilities of the nanocomposites. After exposing the half portion with UV (left hand side picture) sample was immersed in water (right hand side picture) (c). [129] (B) Variation of Young's Modulus with increasing CNC content in the CNC/poly(glycerol sebacate urethane) composite (a). Pictures demonstrating shape memory behavior of the composite with highest CNC loading, originally (b), deformed (c), and after recovery by submersion in water for 1 h (d) [127].

process, the resulting composite also possessed improved fixity and recovery values when compared to neat polyurethane. The neat TPU had a fixity of only 50%, whereas the polyurethane/CNC composite containing 15 wt% CNC had a maximum fixity of 77%; similarly, the recovery of neat TPU was 66% on the first cycle, compared to a 72% recovery for the 15 wt% composite. Similar improvements in fixity were observed by Navarro-Baena et al. [120] when melt-blending CNC into a poly(ε-caprolactone)/poly(ι-lactic acid) polymer composite.

6. Concluding remarks and future prospects

Smart polymers and smart hybrid systems have emerged as powerful next generation materials for a broad range of applications. CNC-based smart hybrid materials are particularly promising, not only because of their remarkable versatility, but also because of their sustainable, biocompatible, and biodegradable nature. Thermo-responsive physically adaptable systems containing CNC benefit not only from the simplicity of their principles, but also from the diversity of potential fabrication approaches and the breadth of applications. By tuning the temperature response of thermo-responsive systems to the biological temperature, a range of biomedical applications become viable. Thermo-responsive CNC systems have also found application as rheological modifiers and fluorescent sensors. Many pH-responsive CNC systems have been developed for use in tunable Pickering emulsions, where the emulsion can be selectively stabilized or destabilized. Additionally, the use of these pH-responsive CNC systems for other applications has been recently explored, such as in industrial flocculation and visual pH sensing. New applications in biomedicine, such as drug delivery and cell culturing, have also drawn increasing attention for all physically adaptable smart CNC systems.

Optically active CNC hybrid systems have also been advanced, allowing for their adoption in a broader range of applications. Through the intercalation of plasticizers, such as glucose, or the incorporation of polymers such as polyurethanes, CNC chiral films are capable of maintaining their longer-range order while also varying their optical properties in response to stimuli such as humidity or strain. This makes the newly developed CNC hybrid materials well suited for a variety of applications, ranging from strain sensors on buildings or bridges to smart printable inks. However, some challenges remain before optically adaptable CNC systems are exploited for scaled-up application. Swelling in the CNC chiral films, whether caused by solvent infiltration or mechanical strain, often leads to progressive disordering of the chiral structures. Generating films that are capable of reorganizing without significant structural erosion between cycles of swelling and shrinking will be important in allowing optically adaptable CNC systems to be used for longer periods of time. Additionally, although CNC systems manipulated to have peak reflectance in the visible light wavelengths have been achieved, there is still much opportunity to explore fabrication methods that can more precisely manipulate the long-range order without being time or energy intensive.

One of the most promising advanced applications of CNC-based smart systems is in self-healing hydrogels. In order to design robust hydrogels, high stiffness is needed, which requires a strong bonding network throughout the material. While this need often conflicts with the high molecular dynamics needed for the self-healing processes, the incorporation of CNC may help satisfy both requirements. Additionally, CNC can be modified to participate only in very specific interactions with self-healing networks, which helps to reduce side interactions that often lead to the passivation of self-healing surfaces.

CNC is also a very promising material for use in shape memory systems. CNC has been successfully employed to improve the mechanical properties of shape memory materials, and functionalized CNC has also been used as the molecular switch component in shape memory systems. Although the incorporation of cellulose in shape memory polymers unilaterally enhances properties, such as modulus of elasticity and maximum strength, it often lowers the composite's elongation at break, limiting the flexibility and wider application of the polymer system. Further study of the interface between CNC and shape memory polymers may help in finding the

optimal balance between improved mechanical strength and flexibility/deformability.

CNCs are currently being produced at an industrial scale in Canada and across the globe, such as in the USA, China, Japan, and Europe. The market potential for CNC in many industrial sectors is enormous, even though the adoption of this sustainable nanomaterial will depend heavily on market forces and economic considerations. As there is a strong motivation through governments and regulators to replace materials derived from fossil fuels with those that are renewable, the use of sustainable nanomaterials will continue to grow. Cellulose nanomaterials in particular offer solutions that balance the competing demands of the environment and financial constraints of consumers.

Declaration of competing interest

The authors declare that they have no known competing financial interests or personal relationships that could have appeared to influence the work reported in this paper.

Acknowledgment

Both MAP and KCT acknowledge the funding from NSERC, Canada.

References

[1] M. Yoshida, J. Lahann, Smart nanomaterials, ACS Nano 2 (6) (2008) 1101–1107.
[2] A.S. Hoffman, 'Intelligent' polymers in medicine and biotechnology, Artif. Organs 19 (5) (1995) 458–467.
[3] M.R. Aguilar, J. San Román, Smart Polymers and Their Applications, Woodhead publishing, 2019.
[4] E. Larsson, et al., Thermoresponsive cryogels reinforced with cellulose nanocrystals, RSC Adv. 5 (95) (2015) 77643–77650.
[5] O. Garcia-Valdez, et al., Grafting CO2-responsive polymers from cellulose nanocrystals via nitroxide-mediated polymerisation, Polym. Chem. 8 (28) (2017) 4124–4131.
[6] O.E. Philippova, et al., pH-responsive gels of hydrophobically modified poly(acrylic acid), Macromolecules 30 (26) (1997) 8278–8285.
[7] J.D. Willott, et al., Hydrophobic effects within the dynamic pH-response of polybasic tertiary amine methacrylate brushes, Phys. Chem. Chem. Phys. 17 (5) (2015) 3880–3890.
[8] M. Thomas, et al., Poly(N,N-dimethylaminoethyl methacrylate) brushes: pH-dependent switching kinetics of a surface-grafted thermoresponsive polyelectrolyte, Langmuir 31 (49) (2015) 13426–13432.
[9] Y. Zhao, T. Ikeda, Smart Light-responsive Materials: Azobenzene-Containing Polymers and Liquid Crystals, John Wiley & Sons, 2009.
[10] I. Cobo, et al., Smart hybrid materials by conjugation of responsive polymers to biomacromolecules, Nat. Mater. 14 (2014) 143.
[11] K.L. Heredia, et al., In situ preparation of Protein-'Smart' polymer conjugates with retention of bioactivity, J. Am. Chem. Soc. 127 (48) (2005) 16955–16960.
[12] M. Karg, T. Hellweg, Smart inorganic/organic hybrid microgels: synthesis and characterisation, J. Mater. Chem. 19 (46) (2009) 8714–8727.
[13] N. Grishkewich, et al., Recent advances in the application of cellulose nanocrystals, Curr. Opin. Colloid Interface Sci. 29 (2017) 32–45.
[14] N. Mohammed, N. Grishkewich, K.C. Tam, Cellulose nanomaterials: promising sustainable nanomaterials for application in water/wastewater treatment processes, Environ. Sci.: Nano 5 (3) (2018) 623–658.
[15] M.S. Islam, et al., Cellulose nanocrystal (CNC)–inorganic hybrid systems: synthesis, properties and applications, J. Mater. Chem. B 6 (6) (2018) 864–883.
[16] I.A. Sacui, et al., Comparison of the properties of cellulose nanocrystals and cellulose nanofibrils isolated from bacteria, tunicate, and wood processed using acid, enzymatic, mechanical, and oxidative methods, ACS Appl. Mater. Interfaces 6 (9) (2014) 6127–6138.
[17] P. Lu, Y.-L. Hsieh, Preparation and properties of cellulose nanocrystals: rods, spheres, and network, Carbohydr. Polym. 82 (2) (2010) 329–336.
[18] P.B. Filson, B.E. Dawson-Andoh, Sono-chemical preparation of cellulose nanocrystals from lignocellulose derived materials, Bioresour. Technol. 100 (7) (2009) 2259–2264.
[19] P. Satyamurthy, et al., Preparation and characterization of cellulose nanowhiskers from cotton fibres by controlled microbial hydrolysis, Carbohydr. Polym. 83 (1) (2011) 122–129.
[20] S. Elazzouzi-Hafraoui, et al., The shape and size distribution of crystalline nanoparticles prepared by acid hydrolysis of native cellulose, Biomacromolecules 9 (1) (2008) 57–65.
[21] B.L. Peng, et al., Chemistry and applications of nanocrystalline cellulose and its derivatives: a nanotechnology perspective, Can. J. Chem. Eng. 89 (5) (2011) 1191–1206.
[22] A. Šturcová, G.R. Davies, S.J. Eichhorn, Elastic modulus and stress-transfer properties of tunicate cellulose whiskers, Biomacromolecules 6 (2) (2005) 1055–1061.
[23] E. Lam, et al., Applications of functionalized and nanoparticle-modified nanocrystalline cellulose, Trends Biotechnol. 30 (5) (2012) 283–290.
[24] M.A.C. Stuart, et al., Emerging applications of stimuli-responsive polymer materials, Nat. Mater. 9 (2010) 101.
[25] S. Dai, P. Ravi, K.C. Tam, Thermo- and photo-responsive polymeric systems, Soft Matter 5 (13) (2009) 2513–2533.
[26] M. Wei, et al., Stimuli-responsive polymers and their applications, Polym. Chem. 8 (1) (2017) 127–143.
[27] O. Kose, et al., Unwinding a spiral of cellulose nanocrystals for stimuli-responsive stretchable optics, Nat. Commun. 10 (1) (2019) 510.
[28] D.Y. Wu, S. Meure, D. Solomon, Self-healing polymeric materials: a review of recent developments, Prog. Polym. Sci. 33 (5) (2008) 479–522.
[29] J. Hu, et al., Recent advances in shape–memory polymers: structure, mechanism, functionality, modeling and applications, Prog. Polym. Sci. 37 (12) (2012) 1720–1763.
[30] M.I. Gibson, R.K. O'Reilly, To aggregate, or not to aggregate? considerations in the design and application of polymeric thermally-responsive nanoparticles, Chem. Soc. Rev. 42 (17) (2013) 7204–7213.
[31] E. Cudjoe, et al., Biomimetic reversible heat-stiffening polymer nanocomposites, ACS Cent. Sci. 3 (8) (2017) 886–894.
[32] J.-M. Malho, et al., Multifunctional stimuli-responsive cellulose nanocrystals via dual surface modification with genetically engineered elastin-like polypeptides and poly(acrylic acid), ACS Macro Lett. 7 (6) (2018) 646–650.
[33] F. Azzam, et al., Preparation by grafting onto, characterization, and properties of thermally responsive polymer-decorated cellulose nanocrystals, Biomacromolecules 11 (12) (2010) 3652–3659.
[34] F. Lin, et al., Temperature-controlled star-shaped cellulose nanocrystal assemblies resulting from asymmetric polymer grafting, ACS Macro Lett. 8 (4) (2019) 345–351.
[35] J. Zhou, et al., Cellulose nanocrystals/fluorinated polyacrylate soap-free emulsion prepared via RAFT-assisted Pickering emulsion polymerization, Colloids Surfaces B Biointerfaces 177 (2019) 321–328.
[36] J. Glasing, et al., Grafting well-defined CO2-responsive polymers to cellulose nanocrystals via nitroxide-mediated polymerisation: effect of graft density and molecular weight on dispersion behaviour, Polym. Chem. 8 (38) (2017) 6000–6012.
[37] N. Grishkewich, et al., Cellulose nanocrystal-poly(oligo(ethylene glycol) methacrylate) brushes with tunable LCSTs, Carbohydr. Polym. 144 (2016) 215–222.
[38] H. Thérien-Aubin, et al., Temperature-responsive nanofibrillar hydrogels for cell encapsulation, Biomacromolecules 17 (10) (2016) 3244–3251.
[39] X. Zhang, et al., Thermoresponsive poly(poly(ethylene glycol) methyl-acrylate)s grafted cellulose nanocrystals through SI-ATRP polymerization, Cellulose 24 (10) (2017) 4189–4203.
[40] J.T. Orasugh, et al., Effect of cellulose nanocrystals on the performance of drug loaded in situ gelling thermo-responsive ophthalmic formulations, Int. J. Biol. Macromol. 124 (2019) 235–245.
[41] X. Sun, et al., Unique thermo-responsivity and tunable optical performance of poly(N-isopropylacrylamide)-cellulose nanocrystal hydrogel films, Carbohydr. Polym. 208 (2019) 495–503.
[42] R. Nigmatullin, et al., Thermosensitive supramolecular and colloidal hydrogels via self-assembly modulated by hydrophobized cellulose nanocrystals, Cellulose 26 (1) (2019) 529–542.
[43] S. Minko, Grafting on solid surfaces: 'grafting to' and 'grafting from' methods, in: M. Stamm (Ed.), Polymer Surfaces and Interfaces: Characterization, Modification and Applications, Springer Berlin Heidelberg, Berlin, Heidelberg, 2008, pp. 215–234.
[44] J.O. Zoppe, et al., Poly(N-isopropylacrylamide) brushes grafted from cellulose nanocrystals via surface-initiated single-electron transfer living radical polymerization, Biomacromolecules 11 (10) (2010) 2683–2691.
[45] W. Wu, et al., Thermo-responsive and fluorescent cellulose nanocrystals grafted with polymer brushes, J. Mater. Chem. 3 (5) (2015) 1995–2005.
[46] K. Zubik, et al., Thermo-responsive poly (N-isopropylacrylamide)-cellulose nanocrystals hybrid hydrogels for wound dressing, Polymers 9 (4) (2017) 119.
[47] Y.R. Lee, et al., Smart cellulose nanofluids produced by tunable hydrophobic association of polymer-grafted cellulose nanocrystals, ACS Appl. Mater. Interfaces 9 (36) (2017) 31095–31101.
[48] E. Gicquel, et al., Tailoring rheological properties of thermoresponsive hydrogels through block copolymer adsorption to cellulose nanocrystals, Biomacromolecules 20 (7) (2019) 2545–2556.

[49] Y. Li, et al., Supramolecular nanofibrillar thermoreversible hydrogel for growth and release of cancer spheroids, Angew. Chem. Int. Ed. 56 (22) (2017) 6083–6087.
[50] J.O. Zoppe, R.A. Venditti, O.J. Rojas, Pickering emulsions stabilized by cellulose nanocrystals grafted with thermo-responsive polymer brushes, J. Colloid Interface Sci. 369 (1) (2012) 202–209.
[51] W. Wu, et al., Temperature-sensitive, fluorescent poly (N-Isopropyl-acrylamide)-Grafted cellulose nanocrystals for drug release, BioResources 11 (3) (2016) 7026–7035.
[52] J. Tang, P.J. Quinlan, K.C. Tam, Stimuli-responsive Pickering emulsions: recent advances and potential applications, Soft Matter 11 (18) (2015) 3512–3529.
[53] A.-L. Oechsle, et al., CO2-Switchable cellulose nanocrystal hydrogels, Chem. Mater. 30 (2) (2018) 376–385.
[54] R. Cha, Z. He, Y. Ni, Preparation and characterization of thermal/pH-sensitive hydrogel from carboxylated nanocrystalline cellulose, Carbohydr. Polym. 88 (2) (2012) 713–718.
[55] J. Fox, et al., High-strength, healable, supramolecular polymer nanocomposites, J. Am. Chem. Soc. 134 (11) (2012) 5362–5368.
[56] Y. Li, et al., Adaptive structured pickering emulsions and porous materials based on cellulose nanocrystal surfactants, Angew Chem. Int. Ed. Engl. 57 (41) (2018) 13560–13564.
[57] W. Du, et al., Heterogeneously modified cellulose nanocrystals-stabilized pickering emulsion: preparation and their template Application for the creation of PS microspheres with amino-rich surfaces, ACS Sustain. Chem. Eng. 5 (9) (2017) 7514–7523.
[58] J. Tang, et al., Dual responsive pickering emulsion stabilized by poly[2-(dimethylamino)ethyl methacrylate] grafted cellulose nanocrystals, Biomacromolecules 15 (8) (2014) 3052–3060.
[59] L.E. Low, et al., Palm olein-in-water Pickering emulsion stabilized by Fe3O4-cellulose nanocrystal nanocomposites and their responses to pH, Carbohydr. Polym. 155 (2017) 391–399.
[60] K.H. Kan, et al., Polymer-grafted cellulose nanocrystals as pH-responsive reversible flocculants, Biomacromolecules 14 (9) (2013) 3130–3139.
[61] Z. Zhang, et al., Gold nanoparticles stabilized by poly(4-vinylpyridine) grafted cellulose nanocrystals as efficient and recyclable catalysts, Carbohydr. Polym. 182 (2018) 61–68.
[62] S. Eyley, et al., CO(2) controlled flocculation of microalgae using pH responsive cellulose nanocrystals, Nanoscale 7 (34) (2015) 14413–14421.
[63] L. Chen, et al., Synthesis and characterization of pH-responsive and fluorescent poly (amidoamine) dendrimer-grafted cellulose nanocrystals, J. Colloid Interface Sci. 450 (2015) 101–108.
[64] M. Rahimi, et al., Biocompatible magnetic tris(2-aminoethyl)amine functionalized nanocrystalline cellulose as a novel nanocarrier for anticancer drug delivery of methotrexate, New J. Chem. 41 (5) (2017) 2160–2168.
[65] N. Li, et al., Fabrication of cellulose-nanocrystal-based folate targeted nanomedicine via layer-by-layer assembly with lysosomal pH-controlled drug release into the nucleus, Biomacromolecules 20 (2) (2019) 937–948.
[66] L. Tang, et al., Synthesis of pH-sensitive fluorescein grafted cellulose nanocrystals with an amino acid spacer, ACS Sustain. Chem. Eng. 4 (9) (2016) 4842–4849.
[67] J. Tang, et al., Polyrhodanine coated cellulose nanocrystals as optical pH indicators, RSC Adv. 4 (104) (2014) 60249–60252.
[68] A.E. Way, et al., pH-responsive cellulose nanocrystal gels and nanocomposites, ACS Macro Lett. 1 (8) (2012) 1001–1006.
[69] L.E. Low, et al., Magnetic cellulose nanocrystal stabilized Pickering emulsions for enhanced bioactive release and human colon cancer therapy, Int. J. Biol. Macromol. 127 (2019) 76–84.
[70] T. Nypelö, et al., Magneto-responsive hybrid materials based on cellulose nanocrystals, Cellulose 21 (4) (2014) 2557–2566.
[71] H. Wang, et al., Dramatically enhanced strain- and moisture-sensitivity of bioinspired fragmentized carbon architectures regulated by cellulose nanocrystals, Chem. Eng. J. 345 (2018) 452–461.
[72] S.-S. Kim, C.-D. Kee, Electro-active polymer actuator based on PVDF with bacterial cellulose nano-whiskers (BCNW) via electrospinning method, Int. J. Precis. Eng. Manuf. 15 (2) (2014) 315–321.
[73] H.-U. Ko, et al., Fabrication and characterization of cellulose nanocrystal based transparent electroactive polyurethane, Smart Mater. Struct. 26 (8) (2017), 085012.
[74] J. Zheng, et al., Polymorphism control of poly(vinylidene fluoride) through electrospinning, Macromol. Rapid Commun. 28 (22) (2007) 2159–2162.
[75] H. Fashandi, et al., Morphological changes towards enhancing piezoelectric properties of PVDF electrical generators using cellulose nanocrystals, Cellulose 23 (6) (2016) 3625–3637.
[76] R. Fu, et al., Improved piezoelectric properties of electrospun poly(vinylidene fluoride) fibers blended with cellulose nanocrystals, Mater. Lett. 187 (2017) 86–88.
[77] L. Han, et al., Self-healable conductive nanocellulose nanocomposites for biocompatible electronic skin sensor systems, ACS Appl. Mater. Interfaces 11 (47) (2019) 44642–44651.
[78] J. Tang, R.M. Berry, K.C. Tam, Stimuli-responsive cellulose nanocrystals for surfactant-free oil harvesting, Biomacromolecules 17 (5) (2016) 1748–1756.
[79] M. Haqani, H. Roghani-Mamaqani, M. Salami-Kalajahi, Synthesis of dual-sensitive nanocrystalline cellulose-grafted block copolymers of N-isopropylacrylamide and acrylic acid by reversible addition-fragmentation chain transfer polymerization, Cellulose 24 (5) (2017) 2241–2254.
[80] W. Yuan, et al., Ultraviolet light-, temperature- and pH-responsive fluorescent sensors based on cellulose nanocrystals, Polym. Chem. 9 (22) (2018) 3098–3107.
[81] J.F. Revol, et al., Helicoidal self-ordering of cellulose microfibrils in aqueous suspension, Int. J. Biol. Macromol. 14 (3) (1992) 170–172.
[82] K.E. Shopsowitz, et al., Free-standing mesoporous silica films with tunable chiral nematic structures, Nature 468 (7322) (2010) 422–425.
[83] X. Mu, D.G. Gray, formation of chiral nematic films from cellulose nanocrystal suspensions is a two-stage process, Langmuir 30 (31) (2014) 9256–9260.
[84] D. Qu, et al., Chiral photonic cellulose films enabling mechano/chemo responsive selective reflection of circularly polarized light, Adv. Opt. Mat. 7 (7) (2019) 1801395.
[85] T.H. Zhao, et al., Printing of responsive photonic cellulose nanocrystal microfilm arrays, Adv. Funct. Mater. 29 (21) (2019) 1804531.
[86] T. Wu, et al., A bio-inspired cellulose nanocrystal-based nanocomposite photonic film with hyper-reflection and humidity-responsive actuator properties, J. Mater. Chem. C 4 (41) (2016) 9687–9696.
[87] Y.-D. He, et al., Biomimetic optical cellulose nanocrystal films with controllable iridescent color and environmental stimuli-responsive chromism, ACS Appl. Mater. Interfaces 10 (6) (2018) 5805–5811.
[88] K. Yao, et al., Flexible and responsive chiral nematic cellulose nanocrystal/poly(ethylene glycol) composite films with uniform and tunable structural color, Adv. Mater. 29 (28) (2017).
[89] H. Wan, et al., Rapidly responsive and flexible chiral nematic cellulose nanocrystal composites as multifunctional rewritable photonic papers with eco-friendly inks, ACS Appl. Mater. Interfaces 10 (6) (2018) 5918–5925.
[90] Y. Cao, et al., Pressure-responsive hierarchical chiral photonic aerogels, Adv. Mater. 31 (21) (2019) 1808186.
[91] O. Kose, et al., Stimuli-responsive anisotropic materials based on unidirectional organization of cellulose nanocrystals in an elastomer, Macromolecules 52 (14) (2019) 5317–5324.
[92] T. Hiratani, et al., Stable and sensitive stimuli-responsive anisotropic hydrogels for sensing ionic strength and pressure, Mater. Horizon 5 (6) (2018) 1076–1081.
[93] C. Sun, et al., Humidity and heat dual response cellulose nanocrystals/poly(N-isopropylacrylamide) composite films with cyclic performance, ACS Appl. Mater. Interfaces 11 (42) (2019) 39192–39200.
[94] B.E. Sørensen, A revised Michel-Lévy interference colour chart based on first-principles calculations, Eur. J. Mineral. 25 (1) (2012) 5–10.
[95] S. Coulibaly, et al., Reinforcement of optically healable supramolecular polymers with cellulose nanocrystals, Macromolecules 47 (1) (2014) 152–160.
[96] G. Xiao, et al., Facile strategy to construct a self-healing and biocompatible cellulose nanocomposite hydrogel via reversible acylhydrazone, Carbohydr. Polym. 218 (2019) 68–77.
[97] M. Zhu, et al., Long-lasting sustainable self-healing ion gel with triple-network by trigger-free dynamic hydrogen bonds and ion bonds, ACS Sustain. Chem. Eng. 6 (12) (2018) 17087–17098.
[98] J.R. McKee, et al., Healable, stable and stiff hydrogels: combining conflicting properties using dynamic and selective three-component recognition with reinforcing cellulose nanorods, Adv. Funct. Mater. 24 (18) (2014) 2706–2713.
[99] L. Cao, et al., Biobased, self-healable, high strength rubber with tunicate cellulose nanocrystals, Nanoscale 9 (40) (2017) 15696–15706.
[100] M.V. Biyani, E.J. Foster, C. Weder, Light-healable supramolecular nanocomposites based on modified cellulose nanocrystals, ACS Macro Lett. 2 (3) (2013) 236–240.
[101] C. Shao, et al., Mussel-Inspired cellulose nanocomposite tough hydrogels with synergistic self-healing, adhesive, and strain-sensitive properties, Chem. Mater. 30 (9) (2018) 3110–3121.
[102] Y.-J. Liu, et al., Ultrasensitive wearable soft strain sensors of conductive, self-healing, and elastic hydrogels with synergistic 'soft and hard' hybrid networks, ACS Appl. Mater. Interfaces 9 (30) (2017) 25559–25570.
[103] L. Bai, et al., Self-healing nanocomposite hydrogels based on modified cellulose nanocrystals by surface-initiated photoinduced electron transfer ATRP, Cellulose 26 (9) (2019) 5305–5319.
[104] L. Cao, et al., A robust and stretchable cross-linked rubber network with recyclable and self-healable capabilities based on dynamic covalent bonds, J. Mater. Chem. 7 (9) (2019) 4922–4933.
[105] C. Shao, et al., Mimicking dynamic adhesiveness and strain-stiffening behavior of biological tissues in tough and self-healable cellulose nanocomposite hydrogels, ACS Appl. Mater. Interfaces 11 (6) (2019) 5885–5895.
[106] W. Li, et al., Self-healing cellulose nanocrystals-containing gels via reshuffling of thiuram disulfide bonds, Polymers 10 (12) (2018) 1392.
[107] W. Huang, et al., On-demand dissolvable self-healing hydrogel based on carboxymethyl chitosan and cellulose nanocrystal for deep partial thickness burn wound healing, ACS Appl. Mater. Interfaces 10 (48) (2018) 41076–41088.
[108] H. Liu, et al., Self-healing and injectable polysaccharide hydrogels with tunable mechanical properties, Cellulose 25 (1) (2018) 559–571.
[109] K. Imato, et al., Dynamic covalent diarylbibenzofuranone-modified nanocellulose: mechanochromic behaviour and application in self-healing polymer composites, Polym. Chem. 8 (13) (2017) 2115–2122.

[110] C. Shao, et al., A self-healing cellulose nanocrystal-poly(ethylene glycol) nanocomposite hydrogel via diels–alder click reaction, ACS Sustain. Chem. Eng. 5 (7) (2017) 6167–6174.
[111] W. Huang, et al., Stretchable, tough, self-recoverable, and cytocompatible chitosan/cellulose nanocrystals/polyacrylamide hybrid hydrogels, Carbohydr. Polym. 222 (2019) 114977.
[112] Q. Meng, J. Hu, A review of shape memory polymer composites and blends, Compos. Appl. Sci. Manuf. 40 (11) (2009) 1661–1672.
[113] C. Liu, H. Qin, P.T. Mather, Review of progress in shape-memory polymers, J. Mater. Chem. 17 (16) (2007) 1543–1558.
[114] M. Behl, A. Lendlein, Shape-memory polymers, Mater. Today 10 (4) (2007) 20–28.
[115] X.-J. Han, et al., pH-induced shape-memory polymers, Macromol. Rapid Commun. 33 (12) (2012) 1055–1060.
[116] Á.. Sonseca, et al., Mechanical and shape-memory properties of poly(-mannitol sebacate)/cellulose nanocrystal nanocomposites, J. Polym. Sci. A Polym. Chem. 52 (21) (2014) 3123–3133.
[117] A. Nicharat, et al., Thermally activated shape memory behavior of melt-mixed polyurethane/cellulose nanocrystal composites, J. Appl. Polym. Sci. 134 (27) (2017) 45033.
[118] F. Pilate, et al., Design of melt-recyclable poly(ε-caprolactone)-based supramolecular shape-memory nanocomposites, RSC Adv. 8 (48) (2018) 27119–27130.
[119] V. Sessini, et al., Effect of the addition of polyester-grafted-cellulose nanocrystals on the shape memory properties of biodegradable PLA/PCL nanocomposites, Polym. Degrad. Stab. 152 (2018) 126–138.
[120] I. Navarro-Baena, J.M. Kenny, L. Peponi, Thermally-activated shape memory behaviour of bionanocomposites reinforced with cellulose nanocrystals, Cellulose 21 (6) (2014) 4231–4246.
[121] A. Shirole, et al., Tailoring the properties of a shape-memory polyurethane via nanocomposite formation and nucleation, Macromolecules 51 (5) (2018) 1841–1849.
[122] A. Saralegi, et al., The role of cellulose nanocrystals in the improvement of the shape-memory properties of castor oil-based segmented thermoplastic polyurethanes, Compos. Sci. Technol. 92 (2014) 27–33.
[123] Z. Wang, et al., Biomass approach toward robust, sustainable, multiple-shape-memory materials, ACS Macro Lett. 5 (5) (2016) 602–606.
[124] M.E. Lamm, et al., Sustainable epoxy resins derived from plant oils with thermo- and chemo-responsive shape memory behavior, Polymer 144 (2018) 121–127.
[125] A. Espinha, et al., Shape memory cellulose-based photonic reflectors, ACS Appl. Mater. Interfaces 8 (46) (2016) 31935–31940.
[126] Y. Liu, et al., Multi-stimulus-responsive shape-memory polymer nanocomposite network cross-linked by cellulose nanocrystals, ACS Appl. Mater. Interfaces 7 (7) (2015) 4118–4126.
[127] T. Wu, et al., Poly(glycerol sebacate urethane)–cellulose nanocomposites with water-active shape-memory effects, Biomacromolecules 15 (7) (2014) 2663–2671.
[128] J. Yang, et al., Water induced shape memory and healing effects by introducing carboxymethyl cellulose sodium into poly(vinyl alcohol), Ind. Eng. Chem. Res. 57 (44) (2018) 15046–15053.
[129] M.V. Biyani, et al., Light-stimulated mechanically switchable, photopatternable cellulose nanocomposites, Polym. Chem. 5 (19) (2014) 5716–5724.
[130] A. Toncheva, et al., Fast IR-actuated shape-memory polymers using in situ silver nanoparticle-grafted cellulose nanocrystals, ACS Appl. Mater. Interfaces 10 (35) (2018) 29933–29942.
[131] Y. Li, et al., pH-responsive shape memory poly(ethylene glycol)–Poly(ε-caprolactone)-based polyurethane/cellulose nanocrystals nanocomposite, ACS Appl. Mater. Interfaces 7 (23) (2015) 12988–12999.
[132] M.L. Auad, et al., Characterization of nanocellulose- reinforced shape memory polyurethanes, Polym. Int. 57 (4) (2008) 651–659.